DOI: 10.1534/genetics.110.115626

Parallel Genetic and Proteomic Screens Identify Msps as a CLASP–Abl Pathway Interactor in Drosophila

L. A. Lowery, H. Lee,[1,2] C. Lu,[2] R. Murphy, R. A. Obar, B. Zhai, M. Schedl, D. Van Vactor[3] and Y. Zhan

Department of Cell Biology, Harvard Medical School, Boston, Massachusetts 02115

Manuscript received February 18, 2010
Accepted for publication May 15, 2010

ABSTRACT

Regulation of cytoskeletal structure and dynamics is essential for multiple aspects of cellular behavior, yet there is much to learn about the molecular machinery underlying the coordination between the cytoskeleton and its effector systems. One group of proteins that regulate microtubule behavior and its interaction with other cellular components, such as actin-regulatory proteins and transport machinery, is the plus-end tracking proteins (MT+TIPs). In particular, evidence suggests that the MT+TIP, CLASP, may play a pivotal role in the coordination of microtubules with other cellular structures in multiple contexts, although the molecular mechanism by which it functions is still largely unknown. To gain deeper insight into the functional partners of CLASP, we conducted parallel genetic and proteome-wide screens for CLASP interactors in *Drosophila melanogaster*. We identified 36 genetic modifiers and 179 candidate physical interactors, including 13 that were identified in both data sets. Grouping interactors according to functional classifications revealed several categories, including cytoskeletal components, signaling proteins, and translation/RNA regulators. We focused our initial investigation on the MT+TIP Minispindles (Msps), identified among the cytoskeletal effectors in both genetic and proteomic screens. Here, we report that Msps is a strong modifier of CLASP and Abl in the retina. Moreover, we show that Msps functions during axon guidance and antagonizes both CLASP and Abl activity. Our data suggest a model in which CLASP and Msps converge in an antagonistic balance in the Abl signaling pathway.

COORDINATION of cytoskeletal dynamics is an essential process for the regulation of virtually all aspects of cellular behavior including cell shape changes, cell division, and cell motility (*e.g.*, Rodriguez *et al.* 2003; Kodama *et al.* 2004). Not only is the cytoskeletal system coordinated with numerous cellular pathways to control cell behavior, it also functions as a central organizing scaffold for multiple effector protein complexes downstream of signaling pathways and cellular processes such as intracellular transport. Yet, little is known regarding the molecular machinery that governs the integrated coordination of various cytoskeletal components. Evidence suggests that the microtubule (MT) plus-end tracking protein CLASP [cytoplasmic linker protein (CLIP)-associated protein], which has been implicated in mitotic spindle formation (Inoue *et al.* 2000, 2004) and in linking MT ends to other cell structures such as the cell cortex and kinetochore (Akhmanova *et al.* 2001; Maiato *et al.* 2003; Mimori-Kiyosue *et al.* 2005; Reis *et al.* 2009), may play a pivotal role in the overall coordination of cytoskeletal networks. Not only does it affect MT dynamics, but CLASP may function as an actin-MT crosslinker as well, as it possesses actin-binding activity (Tsvetkov *et al.* 2007) and CLASP-bound microtubules appear to track along F-actin bundles in growth cones (Lee *et al.* 2004).

We previously showed that CLASP functions downstream of Abelson (Abl) nonreceptor tyrosine kinase (Lee *et al.* 2004), which is a key signaling molecule that modulates the cytoskeleton downstream of numerous cell surface receptor inputs and plays essential roles in various contexts including cell motility and human disease (Van Etten 1999; Moresco and Koleske 2003; Bradley and Koleske 2009). While most cytoskeletal-related studies of Abl have focused on its regulation of actin dynamics (Lanier and Gertler 2000; Wills *et al.* 2002; Hernandez *et al.* 2004; Bradley and Koleske 2009), few studies have examined its MT effectors such as CLASP and how they may be involved in the coordination of both cytoskeletal networks. Additionally, we previously reported that Drosophila *CLASP* is necessary for accurate embryonic axon guidance at the central nervous system (CNS) midline where conserved

Supporting information is available online at http://www.genetics.org/cgi/content/full/genetics.110.115626/DC1.

[1]*Present address:* Department of Life Science, Pohang University of Science and Technology, San31 Hyojadong, Pohang, Kyungbuk, 790-784, Republic of Korea.

[2]These authors contributed equally to this work.

[3]*Corresponding author:* Department of Cell Biology, Harvard Medical School, 240 Longwood Ave., Boston, MA 02115.
E-mail: Davie_vanvactor@hms.harvard.edu

guidance factors (Netrins and Slits) control growth cone navigation (Lee *et al.* 2004). In embryonic axons, we found that *CLASP* is required for *Abl* function (Lee *et al.* 2004); however, additional partner proteins required for *CLASP* activity during axon guidance are largely unknown.

Recent studies of CLASP function focusing on cell culture and imaging have identified several CLASP-binding proteins, such as additional MT+TIPs (CLIP-170 and EB1) (Akhmanova *et al.* 2001; Mimori-Kiyosue *et al.* 2005) and cell cortex-associated proteins (LL5beta and ELKS) (Lansbergen *et al.* 2006). While investigation of the detailed interactions and functional significance of these types of molecules and their relation to CLASP has been important to understanding the CLASP molecular mechanism, elucidating how CLASP functions in a broader context will require expanding our awareness of the entire CLASP network, or "interactome." As of yet, there has not been a comprehensive unbiased survey of CLASP functional interactors.

A long history of molecular pathway dissection in multiple model systems and biological contexts has shown that genetic and proteomic interactome screens are powerful tools for defining the network of functional partners for any given gene of interest (Xu *et al.* 1990; Simon *et al.* 1991; Carthew *et al.* 1994; Karim *et al.* 1996; Rebay *et al.* 2000; St Johnston 2002). Determining the CLASP interaction network can not only define MT+TIP-associated proteins and regulators of MT biology, but it can also reveal new classes of molecules that interact with CLASP. For example, a recent study suggested that CLASPs function as actin-MT crosslinkers because they possess actin-binding activity (Tsvetkov *et al.* 2007), but few specific actin-binding CLASP interactors have been identified, and the functional relevance of CLASP–actin interaction is still unclear. A systematic approach to define the CLASP interactome has the potential for significantly increasing our ability to understand the CLASP mechanism.

Therefore, to expand our knowledge of the CLASP functional mechanism, we have performed a multilevel genetic and proteomic screen for CLASP interactors in Drosophila. The single Drosophila CLASP ortholog has been given multiple names [*orbit/multiple asters* (*MAST*)/*chromosome bows* (*chb*)] (Fedorova *et al.* 1997; Inoue *et al.* 2000; Lemos *et al.* 2000), but here, we refer to it as *CLASP*. Our screen has identified novel and specific partners in several functional categories including cytoskeletal components, signaling proteins, and the unanticipated class of translation/RNA regulators. To validate the findings of this screen, we focused our initial investigation on the conserved MT+TIP identified among the cytoskeletal effectors in both the genetic and proteomic screens, Minispindles (Msps, ortholog of the human CKAP5 [cytoskeleton associated protein 5)/TOG (tumor overexpressed gene)/Xenopus Xmap215)]. Msps function and regulation of MT stability has been studied previously in the context of the mitotic spindle (Cullen *et al.* 1999; Lee *et al.* 2001; Barros *et al.* 2005) and in centrosomes (Popov *et al.* 2002; Cassimeris and Morabito 2004), although it has not been shown to functionally interact with CLASP nor play any role in the nervous system.

Here, we report that Msps is an *in vivo* antagonist of CLASP and interacts strongly with Abl. Furthermore, we show that Msps functions during axon guidance. Our data suggest a model in which CLASP and Msps act antagonistically to provide the growth cone with a rapidly adaptable output for Abl-dependent responses to attractive and repulsive guidance cues.

MATERIALS AND METHODS

Genetic strains, crosses, and manipulation: Flies were cultured on standard media. Crosses were carried out at 25°, except for crosses with the *GMR-GAL4, UAS-Abl* line, which were carried out at 29.5° due to the temperature sensitivity of the Abl retinal phenotype. The following lines were used: the hypomorphic *CLASP* allele *mastp4* (obtained from C. Sunkel and D. Glover), *GMR-GAL4; UAS-Abl* (previously described in Wills *et al.* 2002), *GMR-GAL4, UAS-CLASP-GFP*, *msps*^{P} (Cullen *et al.* 1999), *zipper*^{GD1566} (Dietzl *et al.* 2007), as well as the Exelixis transposon collection (details below). To identify homozygous embryos of the alleles above, the *TM6B Ubx-lacZ* balancer was used (provided by T. Schwarz). For double mutant analyses, *CLASP* and *msps* alleles were combined using lethality and PCR as markers. For gain-of-function analyses, postmitotic, neuron-specific drivers, *elav-GAL4* (present on the third chromosome) or *1407-GAL4* (on the second chromosome) (both described in Luo *et al.* 1994), were used to direct expression of *UAS* transgenes. Both drivers contain the *elav* promoter. *GMR-GAL4* was used to direct expression in the adult retina.

Genetic screening: Two subsets of the Exelixis collection (Artavanis-Tsakonas 2004; Parks *et al.* 2004; Thibault *et al.* 2004) were utilized to screen for genes that modify the fully penetrant, dosage-sensitive, dominant rough eye phenotype resulting from *GMR-GAL4*-directed *CLASP* expression using the *GMR-GAL4, UAS-CLASP-GFP* line. The collection of deletions (Dfs; Parks *et al.* 2004) was used for the primary screen, while the collection of transposon insertions (Thibault *et al.* 2004) was utilized for the secondary screens. The use of these strains for genome-wide genetic interaction screening has been previously described (Kankel *et al.* 2007; Chang *et al.* 2008; Shalaby *et al.* 2009). To confirm candidate interactors, all interacting transposons were crossed in at least two separate experiments to *GMR-GAL4, UAS-CLASP-GFP* and eye phenotypes were examined and imaged. Known CLASP pathway genetic interactors were utilized as positive controls. Because the effect of GAL4 is temperature dependent, and because GMR-GAL4 alone can lead to eye phenotypes, several controls were utilized to account for temperature variability and GAL4 dependence. First, within a given cross, the eye phenotypes of adults with the *GMR-GAL4; UAS-CLASP*; Exel insertion genotype were compared to sibling *GMR-GAL4; UAS-CLASP* flies. These provided an internal control for temperature variability. Furthermore, in every set of crosses performed, several *GMR-GAL4; UAS-CLASP* crosses were also included. Finally, all CLASP-modifying transposon lines were crossed to the *GMR-GAL4* strain to identify insertions that cause CLASP-independent eye phenotypes when misexpressed.

Functional categorization of the candidate interactors was performed using gene ontology information obtained from the following Websites: www.flybase.org, www.ensembl.org,

and www.uniprot.org. Gene ontology analysis was quantified using DAVID2008 (database for annotation, visualization, and integrated discovery) Bioinformatics Resources Web-based tool http://david.abcc.ncifcrf.gov/ (Dennis *et al.* 2003; Huang da *et al.* 2009).

Tandem affinity purification and MS analysis: The full coding region of *CLASP* was cloned into the pMK33-C-TAP vector (Veraksa *et al.* 2005). The construct was shown to be functional by *in vivo* rescue of a *CLASP* LOF mutant. The construct was then transfected into Kc167 cells, and a stable cell line was generated, in addition to one with empty pMK33 vector, by selection in media containing 300 μg/ml hygromycin B (Invitrogen) (Veraksa *et al.* 2005). Cell lines were induced to produce the tandem affinity purification (TAP) fusion protein by treatment with media containing 70 μM cupric sulfate for 16 hr, and the presence of a fusion protein ~180 kDa in the lysate was validated by Western blot. One C-TAP-tagged sample was used without chemical induction to achieve lower levels of CLASP expression. While there was some difference between candidates identified with low *vs.* high levels of expression, there was substantial overlap for the major identified categories. Cells were lysed, and TAP was performed as described previously (Veraksa *et al.* 2005). Peptides were generated from purified samples by in-solution trypsin digestion and analyzed by liquid chromatography–tandem mass spectrometry (LC–MS/MS). The raw MS data was subjected to filtration to remove common contaminants in this type of MS data set (R. A. Obar, unpublished observations). Finally, the individual identified proteins were scored for the number of independent data sets in which they occurred and the numbers of distinct and total peptides for each protein, and this information is noted in supporting information, Table S3. Cytoscape 2.6.3 (Shannon *et al.* 2003) and Xara Xtreme Pro 3.0 software (Xara) was used to construct the interactome figure (Figure 3E).

Immunocytochemistry: Immunocytochemistry and embryonic dissections were performed as described (Van Vactor and Kopczynski 1999). Embryos were incubated in monoclonal 1D4 (anti-FasII) antibody (1:5) overnight at 4°. Rabbit anti-lacZ antibody (MP Biomedicals-Cappel; 1:5000) was used to counterstain embryos from lacZ balancers. Goat anti-mouse HRP and goat anti-rabbit HRP (Jackson ImmunoResearch, 1:500) were used as secondary antibodies. Detection of HRP was performed with the diaminobenzidine substrate peroxidase kit (Vector Laboratories).

Microscopy and image processing: All adult retina images were taken on a Zeiss Stemi SV6 dissecting microscope using a Spot Digital camera and Spot software (Diagnostic Instruments). For immunocytochemistry, images were obtained on a Nikon Eclipse 90i microscope using a Plan Apo ×60/1.40 oil (Nikon) objective, with a DXM1200C Nikon digital camera and NIS Elements (Nikon). Phenotypic quantification was performed from multiple experiments to ensure reproducibility. Figures were prepared using Photoshop CS version 8.0 (Adobe). To statistically compare the axon guidance defects, each segment per embryo was analyzed for defects, and the total number of defective segments per embryo for each genotype was recorded. Statistical analysis was performed with GraphPad InStat software, using the unpaired *t*-test.

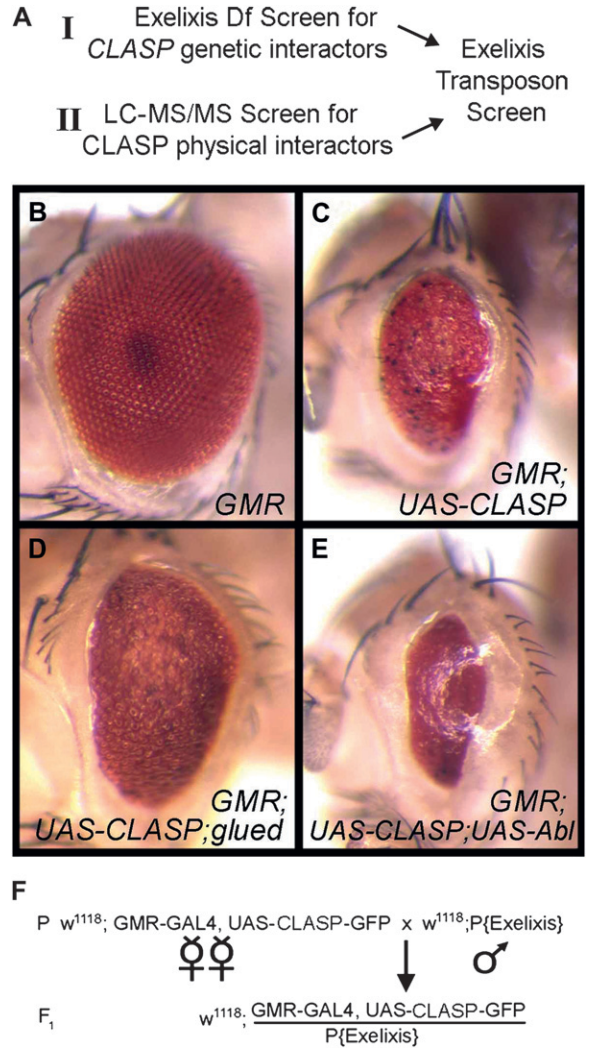

Figure 1.—Multilevel screening design for *CLASP* interactors. (A) Flow chart of screens. (I) Primary genetic screen for Dfs that modify the *GMR-GAL4, UAS-CLASP-GFP* (*GMR-CLASP*) eye phenotype. Interacting Df lines were analyzed for candidate genes within the Df region, and Exelixis transposon lines predicted to interfere with candidate genes were used for second-level genetic screening. (II) In parallel, a mass spectrometry-based proteomic screen was utilized to identify potential physical interactors of CLASP. Transposon lines that corresponded to candidate physical interactors were then tested for genetic interaction with *CLASP*. (B–E) Bright-field micrographs of the Drosophila adult retina. (B) Wild-type retina. (C) *CLASP* overexpression. (D) $glued^{c02410}$ suppresses *CLASP* GOF, making the retina larger. (E) *Abl* GOF enhances *CLASP* GOF, making the retina smaller and glossier. (F) Cross schematic for genetic screening. *GMR-GAL4, UAS-CLASP-GFP* virgin females were crossed to Exelixis transposon insertion males, and F_1 progeny were examined for adult eye phenotypes.

RESULTS

Screening approach for identification of the CLASP interactome in Drosophila: To broadly survey the genome and proteome for novel CLASP interactors (Figure 1A), we have utilized the Drosophila system, where we can combine proteomic tools with different genetic assays that rely upon *in vivo* functional interaction. We adopted a simple and efficient primary genetic screen assay to identify enhancers and suppressors of a GAL4-driven *CLASP* overexpression phenotype in the Drosophila adult retina, using the synthetic *glass*

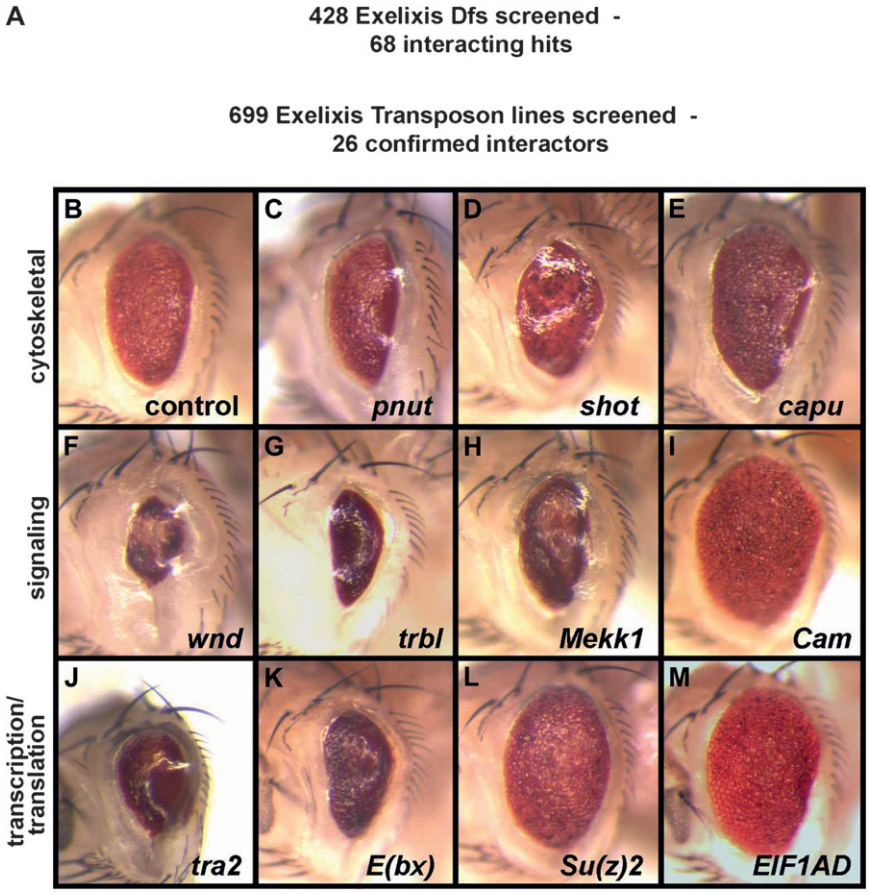

FIGURE 2.—*CLASP* genetic screen interactors. (A) Summary of initial genetic screen including numbers of lines tested for interaction. (B–M) Bright-field micrographs of the Drosophila adult retina show the enhancement or suppression phenotypes of several representatives of *GMR-CLASP* interactors from each functional category. (B) *GMR-CLASP* alone. (C–M) All are transheterozygous for an Exelixis insertion in addition to carrying *GMR-CLASP*.

multiple reporter promoter (GMR) to drive expression in the eye (KARIM *et al.* 1996; THERRIEN *et al.* 2000). Both *CLASP–Abl* and *Abl–robo* interactions were previously detected using this assay (WILLS *et al.* 2002; LEE *et al.* 2004).

Compared to expression of *GMR-GAL4/+* alone (Figure 1B), we observe a rough-eye phenotype when wild-type *CLASP* is overexpressed in the developing compound eye under the control of *GMR-GAL4* (Figure 1C). Several known components of CLASP-associated protein complexes were tested as part of an initial validation of our screen. Double mutant analyses of the *CLASP* retinal gain-of-function (GOF) line combined with loss-of-function (LOF) or GOF mutants of these known interactors shows modification of the retinal phenotype. For example, when *CLASP* is overexpressed in combination with a transposon insertion in the Drosophila dynactin ortholog *glued* (a known interactor of CLASP and +TIP complexes in other systems) (AMARO *et al.* 2008; MANNA *et al.* 2008), suppression of the *CLASP* GOF phenotype occurs (Figure 1D). Conversely, *Abl* GOF shows enhancement of the *CLASP* GOF retinal phenotype (Figure 1E), demonstrating that the adult retinal system is a useful model for identifying genetic interactors of *CLASP*.

A set of reagents for the genetic modifier screen was generously made available to the Drosophila research community by Exelixis in the form of an extensive collection of mapped excision deletions (Dfs) and transposon insertions ideal for identification of genetic modifiers due to its isogenic background (w^{1118}*iso*). While a number of screens have already made use of the Df collection (BONDS *et al.* 2007) or the transposon insertion collection (KANKEL *et al.* 2007; CHANG *et al.* 2008; SHALABY *et al.* 2009) individually, the logistics of obtaining and screening all of the ~16,000 lines is not feasible for many labs. Thus, we applied a hierarchical strategy for our screen (Figure 1A) that would take advantage of both collections and also would assay LOF *vs.* neomorphic effects.

Additionally, we complemented our genetic screen with a proteomic characterization of CLASP-associated proteins in Drosophila, as described below.

Two-level genetic screen identifies 26 interactors of CLASP, including cytoskeletal, signaling, and translation/mRNA regulators: We first screened the Exelixis Df collection to identify the regions of the genome that display LOF genetic interaction with *CLASP* (Figure 1F). From this initial screen of 428 Df lines, we identified 68 interactors of *CLASP*: 42 suppressors and 26 enhancers of the *CLASP* GOF retinal phenotype (Figure 2, Table S1). We followed this with a secondary screen using 699 Exelixis transposon alleles, which corresponded to 376 genes uncovered by the interacting Dfs (Table S2). A caveat to this method is that the Exelixis collections cover ~50% of the genome, and Exelixis transposon

TABLE 1

CLASP genetic screen candidate interactors

Df no. (BL no.)	Insertion no.	CG no.	Gene symbol	Functional category	E/S
7983	d03376, c03283	CG5000	msps	Cytoskeletal	E, S/E
7873	d00747, d03296	CG18076	shot	Cytoskeletal	E, E/E
7539	c04668	CG8704	pnut	Cytoskeletal	S, E
7495	d10743	CG3399	capu	Cytoskeletal	S, S
7543	d09785	CG8472	Cam	Receptors and Signaling	S, S
7615	d03175	CG5408	trbl	Receptors and Signaling	E, E
7944	f00690	CG8789	wnd	Receptors and Signaling	S, E
7660	d01115	CG7717	Mekk1	Receptors and Signaling	E, E
8000	f02193	CG4244	Su(dx)	Receptors and Signaling	S, S
7609	d11255	CG13230	Dab	Receptors and Signaling	E, S
7657	c00535	CG7913	pp2a-b′	Receptors and Signaling	S, S
7495	f05539	CG31957	CG31957	Translation/mRNA regulation	S, S
7749	d10032	CG10128	tra2	Translation/mRNA regulation	S, E
8000	d08252	CG3166	aop	Transcription/DNA binding	S, E
7541	d05100	CG5799	dve	Transcription/DNA binding	S, S
7541	d05100	CG7734	shn	Transcription/DNA binding	S, S
7544	f07746	CG3905	Su(z)2	Transcription/DNA binding	S, S
7563	d02664	CG32346	E(bx)	Transcription/DNA binding	S, E
7510	d01875	CG6287	CG6287	Other: metabolic process	E, S
7543	d09785	CG13167	CG13167	Other: ATPase	S, S
8000	d04217	CG7291	NPC2	Other: lipid/cholesterol	S, S
7510	f07177	CG6258	Rfc38	Other: DNA replication	E, S
7859	d07339	CG8717	slv	Other: RAG1-activating protein	E, E
7549	d10230	CG12758	sano	Unknown	E, E
7882	f00129	CG42524	CG42524	Unknown	S, S
7541	d05100	CG7574	bip1	Unknown	S, S
7543	d09785	CG34021	CG34021	Unknown	S, S
7543	d04917	CG9188	SIP2	Unknown	S, S

BL, Bloomington Stock Center Number; insertion no., Exelixis Deficiency allele name;
E, enhancement of *CLASP* gain-of-function (GOF) phenotype; S, suppression of *CLASP* GOF phenotype. The first letter represents the modification of the Df allele; the second (and third, where applicable) denotes the modification of the transposon insertion allele.

alleles were not available for every possible interacting loci, and thus the screen is not exhaustive. For this reason, we also tested 62 extant alleles that map within positive Dfs (including 29 additional genes) for interaction with CLASP (Table S2).

From this second level of analysis, we identified 12 enhancers and 14 suppressors of *CLASP* (Table 1, Figure 2). Enhancers were defined as those loci that led to smaller eyes and/or with an abnormal surface (either rough or glossy) (Figure 2, C, D, F–H, J, and K) compared to *CLASP* GOF alone (Figure 2B). Suppressors were defined as those loci that led to larger eyes with a more patterned surface (Figure 2, E, I, L, and M). While some of the genetic loci showed the same type of interaction (suppression or enhancement) with both the Df and transposon alleles (in 17 cases), 9 showed opposite effects (Table 1). The transposon insertions in these are in or near the 5′-UTR of the associated loci and contain a UAS element in the correct orientation to drive GAL4-UAS-dependent GOF. Thus, it is likely that the transposon allele led to a neomorphic effect in most of these cases.

Gene ontology (GO) analysis was applied to group the *CLASP*-modifier loci according to functional classifications (MATERIALS AND METHODS). More than half of the loci fell into the following categories: cytoskeletal molecules, signaling molecules, and translation/mRNA and transcription regulators (Table 1). Analysis using the Functional Annotation Chart within the DAVID bioinformatics resources (DENNIS *et al.* 2003; HUANG DA *et al.* 2009) demonstrated that the prevalence of both categories of cytoskeletal molecules and signaling molecules were enriched in the set of *CLASP* interactors compared to their frequency within the entire genome (8-fold and 2.3-fold enrichment, respectively) and these enrichments were statistically significant ($P = 2.8E\text{-}03$ and $1.5E\text{-}2$, respectively).

Within the cytoskeletal group, we identified the MT+TIP *minispindles* (*msps*), the MT+TIP interacting factor, *short stop* (*shot*), as well as the actin-binding proteins *cappuccino* (*capu*, a formin) and *peanut* (*pnut*, a septin). Of these four genes, only *shot* was previously known to interact with *CLASP* (ROGERS *et al.* 2004), and its presence suggests that our genetic screen identified

functionally relevant candidates. Interestingly, like CLASP, the interactors Shot, Capu, and Pnut (which are not known to interact with each other) are all thought to interact with both microfilament and microtubule networks, suggesting that they may be part of the machinery that mediates MT-actin crosstalk.

The largest functional group identified was the signaling molecules, which include both cell surface receptors and numerous intracellular protein kinases and cofactors. Indeed, *calmodulin* (*Cam*) was the most potent suppressor of *CLASP* GOF recovered in this screen, resulting in an eye that is close to wild type in size and with regularity of pattern (Figure 2I). This complements a recent study, which demonstrated that *Cam* and *Abl* interact synergistically to control midline axon guidance in the Drosophila embryonic CNS (Hsouna and Vanberkum 2008) and suggests that Cam, Abl, and CLASP may be part of a concerted mechanism during various developmental processes.

We also observed that the EIF1AD ortholog, *CG31957*, was a very strong suppressor of *CLASP* GOF (Figure 2M). In addition to this gene, with its possible role in translation (it contains a translation initiation factor activity domain), we also identified a gene involved in mRNA regulation and splicing, *tra2* (Figure 2J). *CLASP* has not previously been linked with translation/RNA regulation, but the identification of these two genes points to an intriguing possibility of crosstalk between cytoskeletal regulation and translation. However, the significance of this awaits further investigation.

Combination proteomic–genetic screen for physical interactors of CLASP identifies 13 physical/genetic interactors of CLASP: We complemented our genetic screen with a proteomic characterization of CLASP-associated proteins in Drosophila. Using TAP (Rigaut *et al.* 1999; Bauer and Kuster 2003), we isolated protein complexes associated with TAP-tagged full-length CLASP fusion proteins in Drosophila Kc167 cells (Figure 3, A and B), followed by LC–MS/MS for identification of candidate peptides (Dziembowski and Seraphin 2004; Veraksa *et al.* 2005). Four independent CLASP–TAP purification and LC–MS/MS experiments identified a total of 179 candidate proteins (Table S3). These proteins fell into multiple categories similar to those identified in the initial genetic screen, including cell surface and intracellular signaling proteins, cytoskeletal proteins, and translation/RNA regulators (Figure 3C and Table S3).

Analysis using the DAVID Functional Annotation Chart demonstrated that these three categories were significantly enriched in the proteomic hits compared to the whole genome. First, DAVID analysis confirmed that various signaling pathway members were significantly enriched, such as phosphatases (6.5-fold enrichment, $P = 2.3E\text{-}2$) and GTPases (3.9-fold enrichment, $P = 4.2E\text{-}3$). This was expected as CLASP is downstream of signaling players such as Abl, and indeed, Abl was one of the proteins identified by this proteomic screen, and it also interacts genetically with CLASP (Figure 3, D and E). This indicates that our physical interactor screen identified biologically relevant partners, and it also suggests that CLASP and Abl interact physically, consistent with our previous findings that CLASP is required for Abl function (Lee *et al.* 2004).

DAVID analysis additionally showed that the categories of cytoskeletal proteins and RNA-binding proteins were significantly enriched in our screen compared to the entire genome (4.2-fold enrichment, $P = 3.1E\text{-}5$ and 3.6-fold enrichment, $P = 1.3E\text{-}7$). While numerous proteins involved in metabolism were identified in the mass spectrometry screen, the presence of this group was not identified by DAVID analysis to be statistically significant as these hits were not enriched in our screen compared to the genome.

Upon identifying a set of potential physical interactors of CLASP in Drosophila cells, we then used the Exelixis transposon collection a second time to validate and prioritize the interaction candidates (Figure 1A). We predicted that proteomic candidates that also showed genetic interaction would be particularly important to pursue for further characterization of CLASP pathway functioning. Three of the proteomic hits, Msps, Shot, and Cam, had already been identified in the initial genetic screen. However, many proteomic hits had not been tested for interaction in our first screen. Therefore, we again employed the *in vivo CLASP* interaction assay in the retina to test a total of 190 transposon lines corresponding to 83 of the 179 proteins identified in the proteomic screen (Table S4).

We observed that genes corresponding to 10 additional proteomic candidates showed clear modification of the *CLASP* GOF phenotype (Figure 3D). This secondary screen again highlighted the importance of three classes that were identified in the initial genetic screen (cytoskeletal, intracellular signaling, and translation/RNA regulators) (Figure 3D). Four additional cytoskeletal players (*jar*, *bif*, *kst*, and *CG13366*) and two RNA-related factors, *eIF3-S10* and *Fmr1*, were found to genetically interact with *CLASP*.

One caveat to our screening method was that identifying overlapping proteomic–genetic interaction candidates required the existence of Exelixis insertion lines that corresponded to the mass spectrometry hits. However, this concern could be addressed for particularly interesting-looking candidates that lacked Exelixis lines by genetically screening additional extant alleles. For example, we observed that the nonmuscle myosin Zipper was the most frequently identified candidate that came from the proteomic screen. The Exelixis transposon alleles that might affect *zipper* activity showed only mild interaction with *CLASP* (not shown), presumably because they are weak alleles, and so we also tested for *CLASP* interaction with an independent *zipper* RNAi line *GD1566*. Combining retinal overexpression of *CLASP*

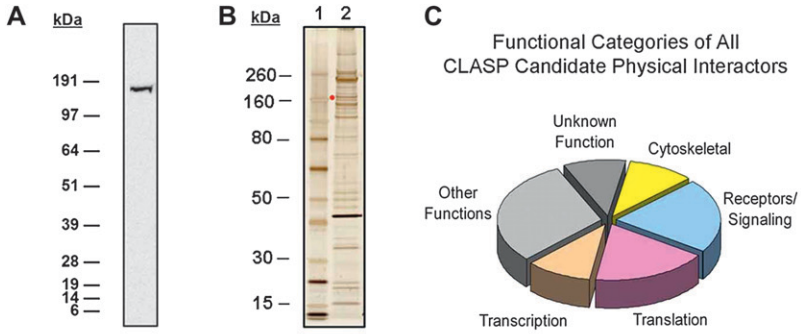

D CLASP Physical Interactors That Also Show Genetic Modification

Symbol	CG #	Name	Predicted function[a]	# Experimental Identifications
zip	CG15792	zipper	cytoskeletal	4
jar	CG5695	jaguar	cytoskeletal	4
CG13366	CG13366	CG13366	cytoskeletal	3
bif	CG1822	bifocal	cytoskeletal	3
kst	CG12008	karst	cytoskeletal	3
shot	CG18076	short stop	cytoskeletal	2
msps	CG5000	mini spindles	cytoskeletal	1
Cam	CG8472	calmodulin	receptors/signaling	4
Abl	CG4032	Abl tyrosine kinase	receptors/signaling	1
CG17272	CG17272	CG17272	receptors/signaling	1
Rab5	CG3664	Rab-protein5	receptors/signaling	1
Fmr1	CG6203	Fmr1	mRNA reg/translation	1
eIF3-S10	CG89805	eIF3-S10	mRNA reg/translation	2

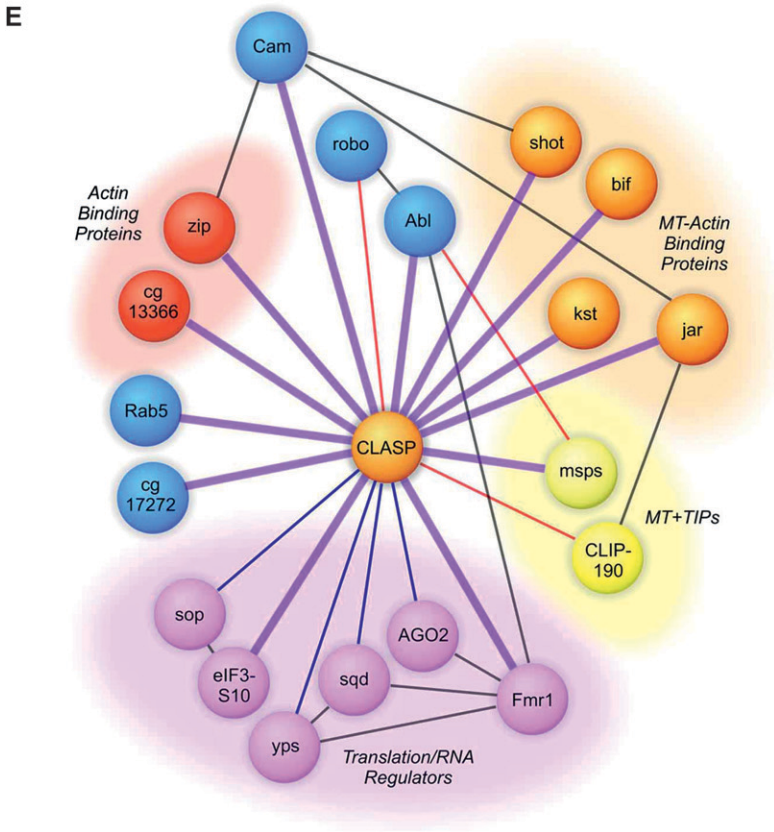

FIGURE 3.—CLASP proteomic screen. (A) The TAP-tagged full-length CLASP clone was transfected into Kc167 cells, and the presence of a fusion protein ~180 kDa in the cell lysate was validated by Western blot. (B) Silver-stained gel of eluate sample from Kc167 cells that stably express C-TAP CLASP illustrates proteins that purify with CLASP (lane 2). The position of the TAP-tagged CLASP bait is marked with a red dot. Lane 1 is protein marker. (C) LC–MS/MS analysis identified 179 candidate physical interactors of CLASP, which fell into several major categories when clustered using ontogeny tools (www.flybase.org; www.ensembl.org; www.ncbi.nlm.nih.gov/sites/entrez?db=gene). (D) Of the 179 candidate interactors, 13 corresponding genes also showed genetic interaction with *CLASP*, and these fell into three categories: cytoskeletal, intracellular signaling, and RNA regulation. (E) CLASP interactome. Thick purple lines indicate interaction supported by both genetic and proteomic data. Blue lines represent physical interaction based on proteomic data, whereas red lines represent genetic interaction. Black lines denote previously known interactions. Blue nodes are components of the receptors/signaling category, pink nodes are mRNA and translation regulators, whereas cytoskeletal components are split into three groups: red are actin-binding proteins, orange are MT-actin binding proteins, and yellow are MT+TIPs[a], based on ontogeny tools.

with knockdown of *zipper* led to a severe eye phenotype (Figure S1). Thus, even proteomic hits that were not yet tested for further genetic interaction may lead to interesting studies in the future.

Our combined genetic and proteomic screens have substantially expanded the CLASP interactome (Figure 3E). Not only have we added to the anticipated networks of signaling and cytoskeletal regulators, providing

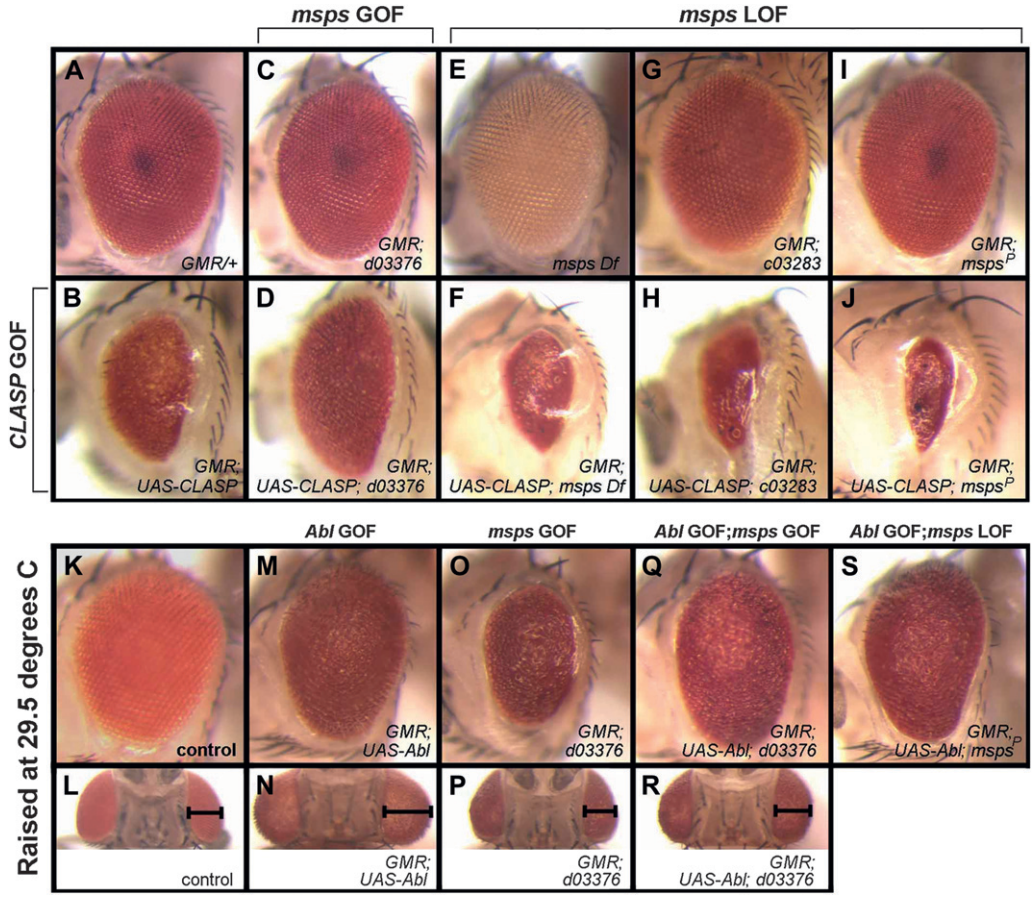

FIGURE 4.—*msps* interacts with both *CLASP* and *Abl* in the adult Drosophila retina. (A) Retina-specific expression of GAL4 (*GMR-GAL4/+*) shows no obvious size or pattern defects. (B) Retinal overexpression of *CLASP* (*GMR-GAL4, UAS-CLASP*) induces a rough eye phenotype. (C) A control shows that the *d03376* allele insertion into the *msps* gene, combined with *GMR-GAL4/+*, has no effect on retinal size or patterning. (D) Coexpression of *CLASP* with one copy of *d03376* shows strong suppression of the eye size phenotype. (E) A control shows that the adult homogygous *Df(3R)Exel7328* (*msps* Df) line, which uncovers the *msps* gene, has no eye size or pattern defects. (F) *Df(3R)Exel7328* heterozygotes (*msps* Df) combined with *CLASP* overexpression enhances the respective eye size defects (compare F and B). (G) A control shows that the *c03283* allele insertion into the *msps* gene, combined with *GMR-GAL4/+*, has no effect on retinal size or patterning. (H) Coexpression of *CLASP* with one copy of *c03283* shows strong enhancement of the eye size phenotype. (I) A control shows that $msps^P$/+ combined with *GMR-GAL4/+*, has no effect on retinal size or patterning, whereas (J) $msps^P$/+ combined with *CLASP* GOF results in strong enhancement. (K) A control sibling raised at 29.5° has a normal size and patterned retina. (L) A control sibling, with eye width denoted by bracket. (M) Retinal overexpression of *Abl* (*GMR-GAL4, UAS-Abl*) induces a rough eye phenotype when raised at 29.5° and an increased retinal field resulting in an eye that bulges outward (N, bracket). (O and P) The *d03376* allele insertion, combined with *GMR-GAL4/+*, also induces a rough eye phenotype when raised at 29.5°. (Q and R) Coexpression of *Abl* with one copy of *d03376* shows suppression of both the *d03376* and *Abl* GOF eye size phenotypes. (S) $msps^P$ LOF heterozygosity also suppresses the *Abl* GOF eye size phenotype. (Q) Retinal overexpression of Abl leads to (R) the *d03376* allele insertion, combined with *GMR-GAL4/+*.

additional players not previously known, but we have discovered unanticipated categories including translation/RNA regulators and actin-binding proteins within the cytoskeletal class of CLASP interactors. The functional relevance of these hits has not yet been tested, but these screens provide a rich source of candidates for further analysis. While future studies examining the translational regulatory genes, for example, may determine new aspects of CLASP functionality, we reasoned that direct insights into the mechanism of CLASP function would come from deeper analysis of its cytoskeletal partners.

msps interacts with both CLASP and Abl: Of the different classes of *CLASP* modifier loci, MT plus-end-associated proteins are of particular interest to us. Specifically, the MT-associated protein Msps was identified in both the genetic and proteomic CLASP interaction screens. Like CLASP, Msps is also a MT+TIP factor (Cullen *et al.* 1999; Lansbergen and Akhmanova 2006). While their overlapping subcellular location suggests a possible association, Msps has not previously been shown to interact physically or functionally with CLASP in any system. Moreover, while CLASP-family proteins have been described as MT "pause" factors (Mimori-Kiyosue *et al.* 2005; Sousa *et al.* 2007) that reduce the dynamics of MT extension and retraction, Msps-family proteins have been called MT "antipause" factors (Brittle and Ohkura 2005), promoting rapid MT dynamics. These reciprocal functions in the regulation of MT dynamics in other systems suggest a possible antagonistic relationship between CLASP and Msps, consistent with the polarity of genetic interaction initially detected in our system.

Because the Exelixis collection contains both LOF and GOF mutations, we first determined whether LOF or GOF of *msps* results in the suppression or enhancement of the *CLASP* GOF phenotype (Figure 4B). The allele of *msps*, which was identified in our genetic screen,

msps^{d03376}, has a UAS site-containing XP transposon within the 5′-UTR of the *msps* gene. Therefore, it is predicted to drive overexpression of Msps in the presence of GAL4. Combining *msps*^{d03376} with *GMR-GAL4*, by itself, does not lead to an eye phenotype (Figure 4C). However, combining *msps*^{d03376} with *GMR-CLASP* leads to a strong suppression of the *CLASP* GOF phenotype (Figure 4D). These data support the presence of an antagonistic relationship between *msps* and *CLASP*, in which gain of *msps* function suppresses *CLASP* GOF.

As GOF effects can sometimes be due to nonphysiological interaction, it was important to validate the functional significance of the *Msps–CLASP* interaction by asking whether *msps* LOF also modified the *CLASP* retinal phenotype. First, we observed that while the *msps* deficiency, *Df(3R)Exel7328*, showed no retinal size or pattern defects over a wild-type chromosome (Figure 4E), combining it with *GMR-CLASP* gives an enhancement of the *CLASP* GOF eye phenotype (*Df(3R)Exel7328/GMR-GAL4, UAS-CLASP*, Figure 4F, compare eye size to 4B). Furthermore, this enhanced phenotype is similar to that seen when combining *GMR-CLASP* with a different *msps* allele predicted to give LOF, *msps*^{c03283} (Figure 4H), in which a PiggyBac transposon without a UAS site is inserted in the 5′ region of the *msps* gene, as well as an extant *msps* hypomorph *msps*^{P} (Figure 4J). This reciprocal phenotypic interaction (*msps* LOF enhancing, and GOF suppressing, the *CLASP* GOF phenotype) further substantiated the antagonistic relationship between Msps and CLASP in the retina.

Although our accumulated evidence shows that CLASP is linked to Abl function during axon guidance, we do not expect all CLASP modifiers to be functionally coupled to the Abl kinase. To determine whether Msps may function with CLASP to support Abl function, we asked whether *msps* also interacts with *Abl* in our retinal assay. Neither *Abl* GOF nor *msps* GOF show a phenotype at 25° (not shown and Figure 4C, respectively), but when the temperature is increased to 29.5° (thus increasing expression levels), both *Abl* and *msps* disrupt retinal development (Figure 4, M and O). While the retina in *Abl* GOF mutants is increased in size, as evidenced by outward bulging of the retina (Figure 4N, bracket), the retinal field in *msps* GOF is reduced (Figure 4O). The combination of both *msps* and *Abl* GOF neutralizes the opposing effects on retinal size, resulting in an eye that is nearly normal in size (Figure 4, Q and R), albeit still abnormal in lens pattern. Interestingly, *msps* LOF also partially suppresses the *Abl* GOF eye phenotype (Figure 4S). Such behavior may be consistent with a multicomponent complex between Msps and Abl or CLASP with a strict stochiometric ratio and fits with the appearance of Abl and Msps in our CLASP physical interaction screen. These Msps interactions are consistent with the cooperative genetic interactions that we previously observed between *CLASP* and *Abl* (Lee *et al.* 2004). This data, combined with the results above, confirmed that Msps functions *in vivo* to genetically modulate the Abl–CLASP pathway and suppress its activation in the Drosophila retina.

msps mutants show axon guidance defects and interaction with CLASP: While the Drosophila retina provided a convenient and efficient means to detect *Msps-CLASP/Abl* interaction, and *Abl* has long been known to be required for normal retinal development (Bennett and Hoffmann 1992), the cellular basis of Abl and CLASP function in the eye is not well understood. Thus, we examined the embryonic nervous system, where Abl's function is well characterized, to determine whether the *Msps–CLASP* interaction is conserved beyond the retina, and to further investigate how Msps and CLASP interact to influence axon pathway formation. Both *CLASP* and *Abl* mutants show axon guidance defects at the CNS midline (Wills *et al.* 2002; Lee *et al.* 2004). Axon fascicles that are restricted to either side of the midline by Slit signaling can be visualized at stage 17 with anti-Fasciclin II (FasII, Mab1D4). In late-stage wild-type and control embryos (stage 17), FasII staining is excluded from the midline and is only present in the three straight, continuous fascicles on either side (Figure 5A). In *CLASP* and *Abl* mutants, ectopic midline crossing occurs, primarily by the midline–proximal MP1 axon pathway (Wills *et al.* 2002; Lee *et al.* 2004), suggesting a failure in the repellent effects of Slit on growth cone orientation.

We first examined embryos for possible CNS defects in the *msps*^{d03376} transposon insertion line, which allows analysis of gain of function. Neuronal overexpression of *msps*, obtained by crossing *msps*^{d03376} to a line containing the postmitotic neuronal driver *elav-GAL4*, led to various lateral longitudinal axonal defects at low penetrance (Figure 5). Not only did we see several cases of axons following ectopic axonal pathways (Figure 5, B and D, arrowheads), we also saw a low penetrance of ectopic midline crossing by the MP1 axon pathway (Figure 5C), similar to *CLASP* and *Abl* mutants. In addition, we occasionally observed missing segments of the third fascicle (Figure 5D, bracket). Some embryos also displayed mildly abnormal wavy fascicles (not shown). These types of defects are consistent with Msps playing a role during axon guidance, and, in particular, an involvement in modulating Slit repulsion, which prevents axons of the longitudinal fascicles from ectopically crossing the midline. Moreover, Slit signaling through a combination of Robo receptors determines the lateral distance of the three longitudinal axon fascicles from the midline (Rajagopalan *et al.* 2000; Simpson *et al.* 2000). Therefore, the inability of *msps* mutants to maintain the proper positioning of their longitudinal axons may reflect a role for Msps in mediating Slit signaling.

To further investigate the role of Msps during axon guidance, we also examined the embryonic CNS in a *msps* loss-of-function allele, *Df(3R)Exel7328*. Compared

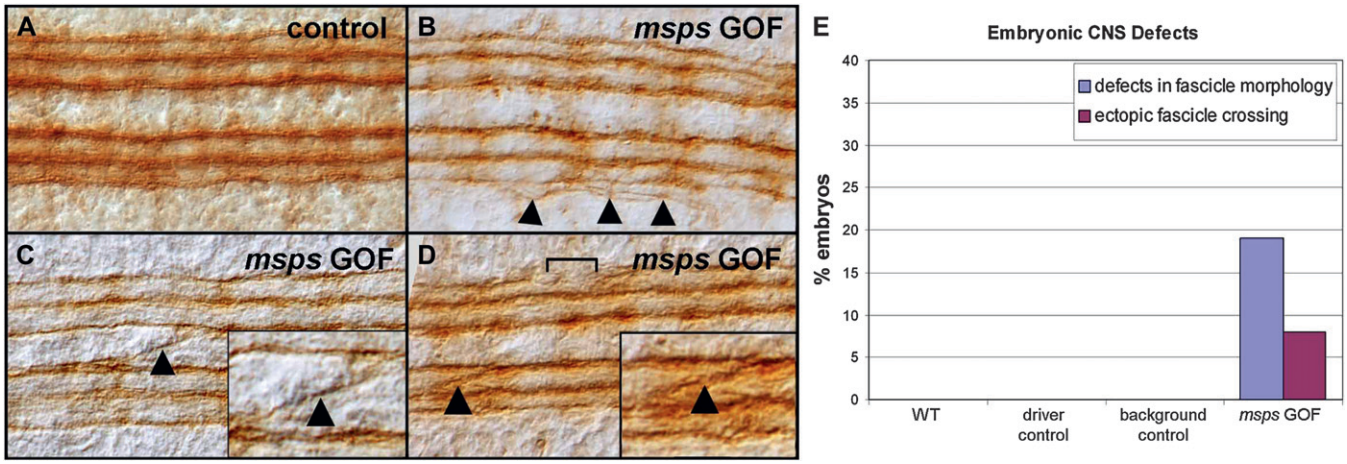

FIGURE 5.—*msps* gain-of-function (GOF) mutants show various embryonic CNS phenotypes. (A) In control *elav-GAL4* embryos, three Fas II-positive axon fascicles can be seen on each side of the midline. (B–D) In *msps* GOF mutants, abnormal phenotypes include ectopic axonal pathways (B, arrowheads), ectopic midline crossing, primarily in the most dorsal–medial MP1 pathway (C, arrowhead and inset), ectopic crossing between other fascicles (D, arrowhead and inset), and regions of missing fascicles (D, bracket). (E) Quantification of the most common axon guidance phenotypes. WT (Canton S) $n = 18$, driver control (*elav-GAL4*) $n = 21$, background control (*d03376/+*) $n = 26$, *msps* GOF (*elav-GAL4/d03376*) $n = 63$.

to control embryos that show three straight fascicles on either side of the midline (Figure 6A), embryos obtained from *msps* Df heterozygotes had axon fascicles with abnormal morphology throughout their longitudinal extent. Not only did some of the axons appear not to be bundled properly, but there were abnormal deflections in the path of the lateral longitudinal tract (Figure 6B), which was stronger than the phenotype observed in *msps* GOF.

While embryos with elevated neuronal CLASP levels also show a low penetrance (11%) of a similar longitudinal fascicle defect (*CLASP* GOF, Figure 6, C and G), neuronal overexpression of *CLASP* combined with the *msps* Df leads to a more severe phenotype (Figure 6, D and G) with a significantly higher penetrance (93%, $P = 0.04$). These data suggest that *msps* and *CLASP* interact functionally during longitudinal axon pathway formation within the embryonic CNS, in an antagonistic fashion that parallels their interaction in the adult retina.

Consistently, we found a similar pattern of interaction when testing for synergy between the *msps* GOF allele *d03376* and the *CLASP* LOF allele *mast^{p4}*. Control embryos of the neuronal driver *1407-GAL4* background show wild-type axonal fascicle morphology, with three straight FasII-positive axon fascicles on either side of the midline (Figure 6A). The embryonic CNS of *CLASP mast^{p4}* mutants shows a moderate penetrance (38%) of ectopic midline crossing (Figure 6, E and H). However, when *mast^{p4}* is combined with *d03376* and neuronal driver *1407-GAL4* to overexpress *msps*, the ectopic midline crossing defect is much more severe, at a higher penetrance (77%) and often affecting numerous segments (Figure 6, F and H). This interaction was highly significant ($P = 0.0007$). Thus, elevation of *msps* in a strong yet partial *CLASP* LOF background further compromises the ability of CLASP to perform its function during midline axon guidance, much as elevation of CLASP exacerbates reduction of Msps function in longitudinal guidance.

We also examined whether *msps* interacts with *Abl* within the context of axon guidance. For this analysis, we examined the ISNb motor axons (Figure 7A) rather than the CNS midline, as Abl acts in both positive and negative capacities during midline guidance (HSOUNA *et al.* 2003; FORSTHOEFEL *et al.* 2005), transducing midline repulsive cues as well as attractive cues, which would complicate interpretation of epistasis experiments. Abl plays a more straightforward role for ISNb motor axons, regulating the extent of ISNb motor-neuron projection into its multiple muscle targets (WILLS *et al.* 1999). First, we observed that *msps* overexpression within the nervous system leads to an ISNb "stop short" phenotype (Figure 7B), which is similar to the phenotype observed in *Abl* LOF mutants (WILLS *et al.* 1999). The opposite phenotype, ISNb "bypass," occurs in *Abl* GOF embryos (Figure 7C). Consistent with *msps* suppression of *Abl* in the retina, overexpression of *msps* in the nervous system completely suppresses the *Abl* ISNb bypass phenotype (Figure 7D, $P < 0.0001$). This indicates that *msps* overexpression can block *Abl* signaling.

DISCUSSION

The *in vivo* functions of cytoskeletal effector and regulatory proteins have been studied very effectively in Drosophila, with particular success at the earliest stages of embryonic development prior to zygotic gene expression, when depletion of maternal stores of such proteins often results in disruption of mitosis, cellularization, or other aspects of cell biology (*e.g.*, SCHEJTER

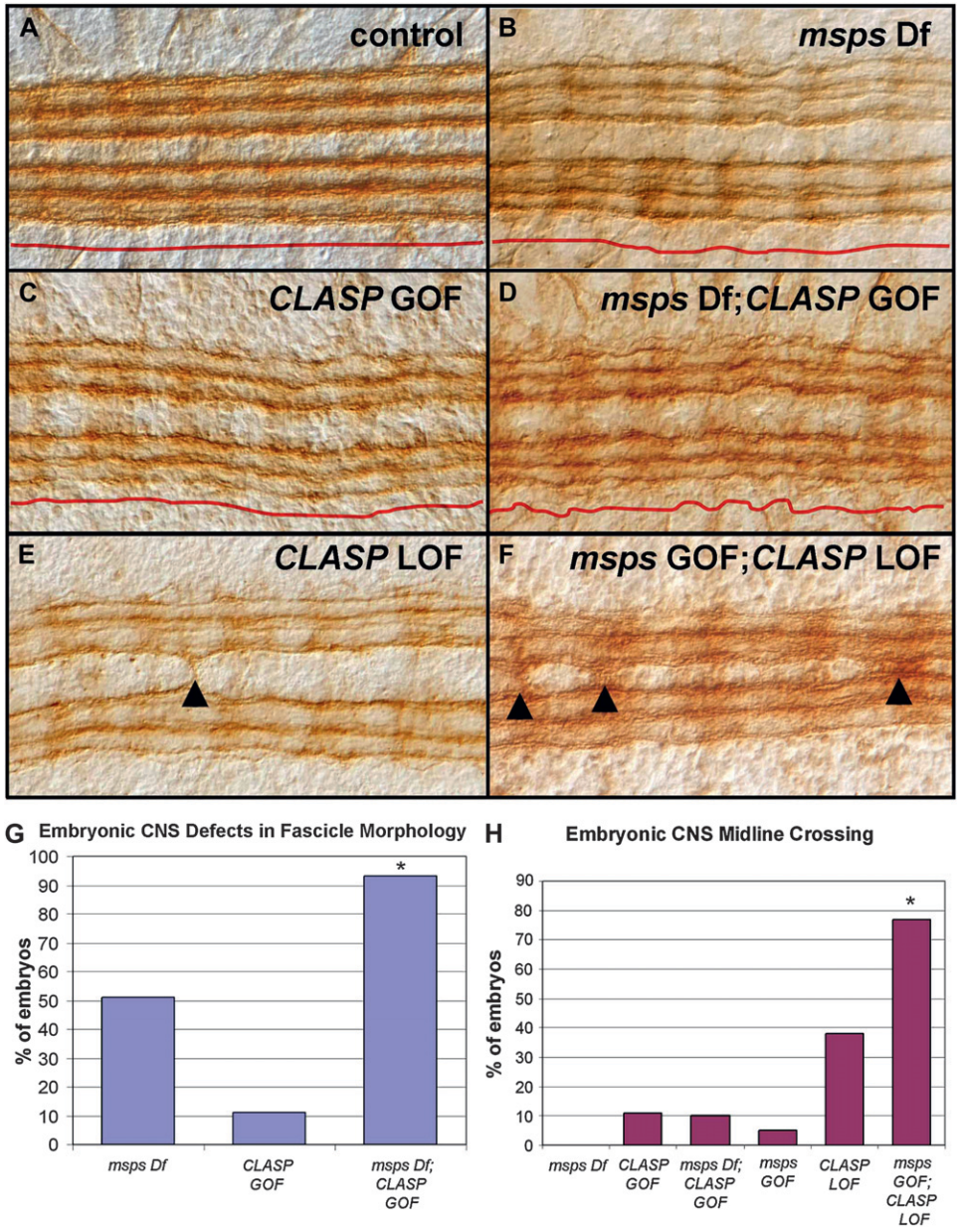

FIGURE 6.—*msps* shows genetic interaction with *CLASP* in the embryonic CNS. (A) In control *elav-GAL4* embryos, three straight Fas II-positive axon fascicles can be seen on each side of the midline. Red line below stained fascicles shows tracing of fascicle directly above it (also in B–D). (B) In *msps* Df embryos, defects in axonal fascicle morphology are apparent, which include axons that do not bundle correctly, as well as axons and fascicles that are abnormally wavy in their pathfinding. (C) *CLASP* GOF mutants also show mild fascicle morphology defects in ~10% of embryos. (D) *msps Df; CLASP* GOF embryos show more severe fascicle morphology defects at >90% penetrance. (E) *CLASP* LOF mutants have ectopic midline crossing (arrowhead). (F) *msps* GOF; *CLASP* LOF double mutants display increased midline crossing compared to *CLASP* LOF alone. (G and H) Quantification of embryonic CNS fascicle defects (G) and ectopic midline crossing (H) demonstrates that *msps* Df; *CLASP* GOF embryos show interaction for fascicle defects ($P = 0.04$), while *msps* GOF; *CLASP* LOF mutants show synergy for ectopic midline crossing ($P = 0.0007$). *msps* Df [*Df(3R)Exel7328*] $n = 43$, *CLASP* GOF (*1407-GAL4/UAS-CLASP*) $n = 9$, *msps* Df; *CLASP* GOF *[1407-GAL4/UAS-CLASP; Df(3R)Exel7328]* $n = 41$, *msps* GOF *(1407-GAL4/+;d03376/+)* $n = 63$, *CLASP LOF* ($mast^{b4}/mast^{b4}$) $n = 21$, *msps* GOF; CLASP LOF (*1407-GAL4/+; d03376,* $mast^{b4}/mast^{b4}$) $n = 13$.

and WIESCHAUS 1993). However, the functions of cytoskeletal effectors at late stages of development are often obscured by early embryonic functions. In this regard, the existence of maternal stores of some key effectors has been helpful for analysis of late events in nervous system development, such as axonal and dendritic patterning, because such maternal supplies of protein are sometimes exhausted only at late stages when axons and dendrites emerge (*e.g.*, WILLS *et al.* 1999). However, zygotic mutations in many key cytoskeletal components disrupt early stages, making screens based on neuroanatomical phenotypes problematic. For this reason, we have utilized genetic interaction screens to explore the network of cytoskeletal regulators linked to key guidance signaling molecules as a means of identifying candidates for deeper analysis during axonal development. Our screens for modifiers of Abl kinase phenotypes led to the identification of CLASP as an effector essential for accurate growth cone navigation (LEE *et al.* 2004). By using CLASP as a starting point for a new generation of screens, we have defined new functional categories and individual players of the CLASP interactome, including cytoskeletal components, signaling proteins, and translation/RNA regulators. In addition, we have identified a microtubule regulatory protein (the MT+TIP Msps) not previously associated with axonal pathfinding decisions.

To build functional neural networks, axonal growth cones must accurately interpret and translate multiple guidance cues into directional movement by coordinating both microtubule and F-actin networks (LOWERY and VAN VACTOR 2009). There appears to be significant

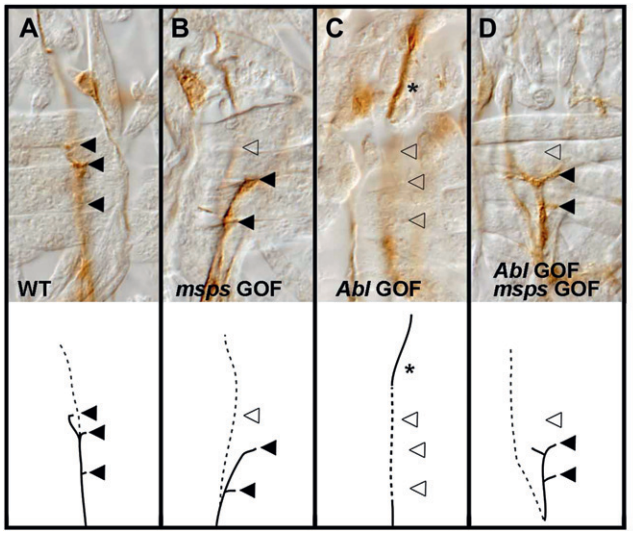

Figure 7.—Overexpression of *msps* suppresses *Abl* axon guidance phenotype. (A) In late-stage WT embryos, ISNb innervates the clefts between muscles 6, 7, 12, and 13 normally (arrowheads). (B) In embryos overexpressing msps (*1407-GAL4; d03376*), ISNb sometimes fails to reach its final muscle target (open arrowhead), generating a "stop short" phenotype. (C) In embryos overexpressing *Abl* (*1407-GAL4; UAS-Abl*), ISNb sometimes fails to innervate its target muscles and instead follows ISN, leading to a "bypass" phenotype (asterisk). Note that the bypass axon is out of the focal plane of muscles 6 and 7. (D) The ISNb bypass phenotype of *Abl* GOF is suppressed when *msps* is also overexpressed (*1407-GAL4; UAS-Abl/d03376*). (D) Quantification of the ISNb bypass phenotype shows that bypass is completely suppressed ($P < 0.0001$) in embryos with overexpressed *msps* and *Abl* compared to *Abl* GOF alone (*1407-GAL4; d03376* $n = 101$*; 1407-GAL4; UAS-Abl*, $n = 106$; *1407-GAL4; UAS-Abl/d03376*, $n = 95$).

interplay between the two cytoskeletal components (Schaefer *et al.* 2002), but we do not yet have a sophisticated understanding of the signaling and effector mechanisms by which both systems are coordinated in response to guidance cues. The Abl tyrosine kinase is one of the few known signaling molecules shown to transduce guidance cue signals to both actin and MT networks (Lanier and Gertler 2000; Wills *et al.* 2002; Lee *et al.* 2004; Hernandez *et al.* 2004; Bradley and Koleske 2009), although far less is known regarding how it regulates MTs. Our work, and that of others, suggests that CLASP may be an important player in the MT-actin crosstalk machinery.

The largest thematic group of CLASP-interacting genes we identified is the actin-binding proteins, including Shot, Zip, Capu, Pnut, Jar, Bif, Kst, and the uncharacterized CG13366 (ortholog of calponin-homology domain containing CYTSA/B). These are all known actin-associated factors that are also predicted to bind to MTs, and their presence in our screen points to a role for CLASP in mediating actin dynamics in coordination with the MT network. This supports previous observations that vertebrate CLASPs may function as actin–MT crosslinkers. CLASPs possess actin-binding activity (Tsvetkov *et al.* 2007), and CLASP-decorated MT tips track along actin filament bundles in the growth cone peripheral domain (Lee *et al.* 2004). Moreover, CLASP was recently shown to bind to the actin-binding protein, IQGAP1, and phosphorylation of CLASP controls linkage of MTs to actin through IQGAP1 for cell migration (Watanabe *et al.* 2009). From our work, it appears that CLASP may have numerous other effector proteins that can modulate its interaction with the actin network. IQGAPs have not been found in Drosophila, and so, we speculate that the novel interactors we identified, as well as others, may allow CLASP to link MTs and actin in different contexts.

The novel CLASP MT+TIP interactor that we identified, Msps, emerged from our screens as a high priority for future analysis. Msps interacts with CLASP in both the genetic and proteomic screens, and it antagonizes CLASP and Abl signaling. The antagonism seen between Msps and CLASP in the Drosophila retina is consistent with cell culture studies, which have shown that CLASP regulates MT dynamics by specifically promoting the pause state (Sousa *et al.* 2007) whereas Msps-family proteins function as MT antipause factors (Brittle and Ohkura 2005). More specifically, CLASPs have MT-stabilizing effects (Drabek *et al.* 2006), and depleting cells of CLASP protein results in highly dynamic, constantly growing or shrinking MTs (Sousa *et al.* 2007). Alternatively, Msps family members can have the opposite effect (Popov and Karsenti 2003), catalyzing the addition and removal of multiple tubulin dimers at MT plus-ends (Brouhard *et al.* 2008), and depletion of Msps results in a dramatic increase in MT pausing with little or no growth (Brittle and Ohkura 2005). These opposite effects on MT behavior in cell culture studies suggest reciprocal functions in the regulation of MT dynamics *in vivo*, and Msps could thus be a component of the Abl signaling pathway that provides an antagonistic counterbalance to CLASP in regulating the growth cone cytoskeletal output downstream of guidance cues.

In the context of CNS, it seems likely that CLASP and Msps drive axon guidance decisions through reciprocal regulation of growth cone turning toward or away from the source of axon guidance factors at the midline. Accurate navigation of both ipsilateral and contralateral axon pathways requires a combination of cues, to

regulate both midline crossing behavior and also the stereotyped positions of longitudinal axon tracts (Evans and Bashaw 2010). The lateral specification model proposes that for longitudinal axons to find and maintain a correct trajectory at a specific distance from the midline, they must reach a balance of turning responses to the attractive Netrins and repellent Slit secreted by midline glia (Rajagopalan *et al.* 2000; Simpson *et al.* 2000; Killeen and Sybingco 2008). Perhaps this balance requires antagonism of Msps and CLASP downstream of Abl, such that reduction of either protein would bias the growth cone or reduce the fidelity of the overall navigation process. Abl has been shown to mediate both Slit and Netrin activity (Wills *et al.* 2002; Forsthoefel *et al.* 2005), thus providing a potential point of integration.

While we anticipate that CLASP and Msps will influence the directionality of growth cone advance in response to guidance cues, the cellular mechanism by which these two effectors guide axons is not yet known. Reciprocal control over MT advance toward the growth cone peripheral domain could account for the effects of CLASP and Msps. However, there are alternatives. For example, reciprocal modulation of growth cone cell adhesion by Msps and CLASP might underlie the two phenotypes we observe in the different mutants. Reduction of adhesion has already been shown to be key in the midline repulsive response to Robo (Rhee *et al.* 2002), whereas an increase in adhesion has long been known to be vital for fasciculation (Rutishauser 1985; Landmesser *et al.* 1988). Interestingly, the Abl kinase that interacts with both Msps and CLASP was also implicated in Robo-dependent modulation of cell adhesion (Rhee *et al.* 2002). If CLASP were to play a role in Robo-mediated suppression of adhesion, then the ectopic midline crossing that occurs in *CLASP* LOF mutants could be explained by an increase in growth cone adhesion toward the midline, which is exacerbated when Msps is overexpressed. Consistently, the fasciculation morphology defects that occur in *msps* LOF (and are exacerbated by *CLASP* GOF) could be explained if the role of Msps is to promote adhesion. Although the effects of CLASP-family proteins on cell adhesion have not been directly measured, studies in nonneuronal contexts suggest that CLASP helps to drive MT–cortical interactions, which would presumably promote, not suppress, adhesion (Mimori-Kiyosue *et al.* 2005).

In conclusion, this is the first study demonstrating that Msps functions during axon guidance. Numerous studies have analyzed its role in the regulation of MT stability in several systems including the mitotic spindle (Cullen *et al.* 1999; Lee *et al.* 2001; Barros *et al.* 2005) and in centrosomes (Popov *et al.* 2002; Cassimeris and Morabito 2004), but its potential role(s) in the nervous system has never been previously addressed. In fact, the growth cone functions of most MT+TIPs are unknown; however, previous discoveries that MT+TIPs CLASP and APC, and now Msps, are important for axon guidance demonstrates that the MT+TIPs are an exciting class of guidance effectors worthy of further exploration and understanding (Lee *et al.* 2004; Zhou and Cohan 2004).

We thank Spyros Artavanis-Tsakonas, as well as members of the Van Vactor lab, for helpful discussions and constructive criticism, and Emily McKillip for technical assistance. We thank Exelixis for donating the collection and the robotics necessary for its maintenance, and we are deeply grateful to the Artavanis-Tsakonas lab for supplying the lines. We thank Steve Gygi and the Gygi Lab Taplin Biological Mass Spectrometry facility for technical expertise and use of the facility. We also thank C. Sunkel, D. Glover, and T. Schwarz for providing published reagents. We thank the Bloomington Drosophila Stock Center and the Vienna Drosophila RNAi Center for fly stocks. L.A.L. is supported by a National Institutes of Health (NIH) National Research Service Award postdoctoral fellowship. D.V.V. is supported by a grant from the NIH (NS-035909). R.A.O. was supported by an NIH grant (HG-003616) and the Javitz Foundation.

LITERATURE CITED

Akhmanova, A., C. C. Hoogenraad, K. Drabek, T. Stepanova, B. Dortland *et al.*, 2001 Clasps are CLIP-115 and -170 associating proteins involved in the regional regulation of microtubule dynamics in motile fibroblasts. Cell **104:** 923–935.

Amaro, I. A., M. Costanzo, C. Boone and T. C. Huffaker, 2008 The *Saccharomyces cerevisiae* homolog of p24 is essential for maintaining the association of p150Glued with the dynactin complex. Genetics **178:** 703–709.

Artavanis-Tsakonas, S., 2004 Accessing the Exelixis collection. Nat. Genet. **36:** 207.

Barros, T. P., K. Kinoshita, A. A. Hyman and J. W. Raff, 2005 Aurora A activates D-TACC-Msps complexes exclusively at centrosomes to stabilize centrosomal microtubules. J. Cell Biol. **170:** 1039–1046.

Bauer, A., and B. Kuster, 2003 Affinity purification-mass spectrometry. Powerful tools for the characterization of protein complexes. Eur. J. Biochem. **270:** 570–578.

Bennett, R. L., and F. M. Hoffmann, 1992 Increased levels of the Drosophila Abelson tyrosine kinase in nerves and muscles: subcellular localization and mutant phenotypes imply a role in cell-cell interactions. Development **116:** 953–966.

Bonds, M., J. Sands, W. Poulson, C. Harvey and T. Von Ohlen, 2007 Genetic screen for regulators of ind expression identifies shrew as encoding a novel twisted gastrulation-like protein involved in Dpp signaling. Dev. Dyn. **236:** 3524–3531.

Bradley, W. D., and A. J. Koleske, 2009 Regulation of cell migration and morphogenesis by Abl-family kinases: emerging mechanisms and physiological contexts. J. Cell Sci. **122:** 3441–3454.

Brittle, A. L., and H. Ohkura, 2005 Mini spindles, the XMAP215 homologue, suppresses pausing of interphase microtubules in Drosophila. EMBO J. **24:** 1387–1396.

Brouhard, G. J., J. H. Stear, T. L. Noetzel, J. Al-Bassam, K. Kinoshita *et al.*, 2008 XMAP215 is a processive microtubule polymerase. Cell **132:** 79–88.

Carthew, R. W., T. P. Neufeld and G. M. Rubin, 1994 Identification of genes that interact with the sina gene in Drosophila eye development. Proc. Natl. Acad. Sci. USA **91:** 11689–11693.

Cassimeris, L., and J. Morabito, 2004 TOGp, the human homolog of XMAP215/Dis1, is required for centrosome integrity, spindle pole organization, and bipolar spindle assembly. Mol. Biol. Cell **15:** 1580–1590.

Chang, H. C., D. N. Dimlich, T. Yokokura, A. Mukherjee, M. W. Kankel *et al.*, 2008 Modeling spinal muscular atrophy in Drosophila. PLoS One **3:** e3209.

Cullen, C. F., P. Deak, D. M. Glover and H. Ohkura, 1999 mini spindles: a gene encoding a conserved microtubule-associated protein required for the integrity of the mitotic spindle in Drosophila. J. Cell Biol. **146:** 1005–1018.

Dennis, Jr., G., B. T. Sherman, D. A. Hosack, J. Yang, W. Gao *et al.*, 2003 DAVID: Database for Annotation, Visualization, and Integrated Discovery. Genome Biol. **4:** 3.

Dietzl, G., D. Chen, F. Schnorrer, K. C. Su, Y. Barinova *et al.*, 2007 A genome-wide transgenic RNAi library for conditional gene inactivation in Drosophila. Nature **448:** 151–156.

Drabek, K., M. van Ham, T. Stepanova, K. Draegestein, R. van Horssen *et al.*, 2006 Role of CLASP2 in microtubule stabilization and the regulation of persistent motility. Curr. Biol. **16:** 2259–2264.

Dziembowski, A., and B. Seraphin, 2004 Recent developments in the analysis of protein complexes. FEBS Lett. **556:** 1–6.

Evans, T. A., and G. J. Bashaw, 2010 Axon guidance at the midline: of mice and flies. Curr. Opin. Neurobiol. **20:** 79–85.

Fedorova, S. A., V. L. Chubykin, A. M. Gucachenko and L. V. Omel'ianchuk, 1997 Mutation chromosome bows (chb-v40), inducing the abnormal chromosome spindle in Drosophila melanogaster. Genetika **33:** 1502–1509.

Forsthoefel, D. J., E. C. Liebl, P. A. Kolodziej and M. A. Seeger, 2005 The Abelson tyrosine kinase, the Trio GEF and Enabled interact with the Netrin receptor Frazzled in Drosophila. Development **132:** 1983–1994.

Hernandez, S. E., J. Settleman and A. J. Koleske, 2004 Adhesion-dependent regulation of p190RhoGAP in the developing brain by the Abl-related gene tyrosine kinase. Curr. Biol. **14:** 691–696.

Hsouna, A., Y. S. Kim and M. F. VanBerkum, 2003 Abelson tyrosine kinase is required to transduce midline repulsive cues. J. Neurobiol. **57:** 15–30.

Hsouna, A., and M. F. VanBerkum, 2008 Abelson tyrosine kinase and Calmodulin interact synergistically to transduce midline guidance cues in the Drosophila embryonic CNS. Int. J. Dev. Neurosci. **26:** 345–354.

Huang da, W., B. T. Sherman and R. A. Lempicki, 2009 Systematic and integrative analysis of large gene lists using DAVID bioinformatics resources. Nat. Protoc. **4:** 44–57.

Inoue, Y. H., M. do Carmo Avides, M. Shiraki, P. Deak, M. Yamaguchi *et al.*, 2000 Orbit, a novel microtubule-associated protein essential for mitosis in Drosophila melanogaster. J. Cell Biol. **149:** 153–166.

Inoue, Y. H., M. S. Savoian, T. Suzuki, E. Mathe, M. T. Yamamoto *et al.*, 2004 Mutations in orbit/mast reveal that the central spindle is comprised of two microtubule populations, those that initiate cleavage and those that propagate furrow ingression. J. Cell Biol. **166:** 49–60.

Kankel, M. W., G. D. Hurlbut, G. Upadhyay, V. Yajnik, B. Yedvobnick *et al.*, 2007 Investigating the genetic circuitry of mastermind in Drosophila, a notch signal effector. Genetics **177:** 2493–2505.

Karim, F. D., H. C. Chang, M. Therrien, D. A. Wassarman, T. Laverty *et al.*, 1996 A screen for genes that function downstream of Ras1 during Drosophila eye development. Genetics **143:** 315–329.

Killeen, M. T., and S. S. Sybingco, 2008 Netrin, Slit and Wnt receptors allow axons to choose the axis of migration. Dev. Biol. **323:** 143–151.

Kodama, A., T. Lechler and E. Fuchs, 2004 Coordinating cytoskeletal tracks to polarize cellular movements. J. Cell Biol. **167:** 203–207.

Landmesser, L., L. Dahm, K. Schultz and U. Rutishauser, 1988 Distinct roles for adhesion molecules during innervation of embryonic chick muscle. Dev. Biol. **130:** 645–670.

Lanier, L. M., and F. B. Gertler, 2000 From Abl to actin: Abl tyrosine kinase and associated proteins in growth cone motility. Curr. Opin. Neurobiol. **10:** 80–87.

Lansbergen, G., and A. Akhmanova, 2006 Microtubule plus end: a hub of cellular activities. Traffic **7:** 499–507.

Lansbergen, G., I. Grigoriev, Y. Mimori-Kiyosue, T. Ohtsuka, S. Higa *et al.*, 2006 CLASPs attach microtubule plus ends to the cell cortex through a complex with LL5beta. Dev. Cell **11:** 21–32.

Lee, H., U. Engel, J. Rusch, S. Scherrer, K. Sheard *et al.*, 2004 The microtubule plus end tracking protein Orbit/MAST/CLASP acts downstream of the tyrosine kinase Abl in mediating axon guidance. Neuron **42:** 913–926.

Lee, M. J., F. Gergely, K. Jeffers, S. Y. Peak-Chew and J. W. Raff, 2001 Msps/XMAP215 interacts with the centrosomal protein D-TACC to regulate microtubule behaviour. Nat. Cell. Biol. **3:** 643–649.

Lemos, C. L., P. Sampaio, H. Maiato, M. Costa, L. V. Omel'yanchuk *et al.*, 2000 Mast, a conserved microtubule-associated protein required for bipolar mitotic spindle organization. EMBO J. **19:** 3668–3682.

Lowery, L. A., and D. Van Vactor, 2009 The trip of the tip: understanding the growth cone machinery. Nat. Rev. Mol. Cell. Biol. **10:** 332–343.

Luo, L., Y. J. Liao, L. Y. Jan and Y. N. Jan, 1994 Distinct morphogenetic functions of similar small GTPases: Drosophila Drac1 is involved in axonal outgrowth and myoblast fusion. Genes Dev. **8:** 1787–1802.

Maiato, H., E. A. Fairley, C. L. Rieder, J. R. Swedlow, C. E. Sunkel *et al.*, 2003 Human CLASP1 is an outer kinetochore component that regulates spindle microtubule dynamics. Cell **113:** 891–904.

Manna, T., S. Honnappa, M. O. Steinmetz and L. Wilson, 2008 Suppression of microtubule dynamic instability by the +TIP protein EB1 and its modulation by the CAP-Gly domain of p150glued. Biochemistry **47:** 779–786.

Mimori-Kiyosue, Y., I. Grigoriev, G. Lansbergen, H. Sasaki, C. Matsui *et al.*, 2005 CLASP1 and CLASP2 bind to EB1 and regulate microtubule plus-end dynamics at the cell cortex. J. Cell Biol. **168:** 141–153.

Moresco, E. M., and A. J. Koleske, 2003 Regulation of neuronal morphogenesis and synaptic function by Abl family kinases. Curr. Opin. Neurobiol. **13:** 535–544.

Parks, A. L., K. R. Cook, M. Belvin, N. A. Dompe, R. Fawcett *et al.*, 2004 Systematic generation of high-resolution deletion coverage of the Drosophila melanogaster genome. Nat. Genet. **36:** 288–292.

Popov, A. V., and E. Karsenti, 2003 Stu2p and XMAP215: turncoat microtubule-associated proteins? Trends Cell Biol. **13:** 547–550.

Popov, A. V., F. Severin and E. Karsenti, 2002 XMAP215 is required for the microtubule-nucleating activity of centrosomes. Curr. Biol. **12:** 1326–1330.

Rajagopalan, S., V. Vivancos, E. Nicolas and B. J. Dickson, 2000 Selecting a longitudinal pathway: Robo receptors specify the lateral position of axons in the Drosophila CNS. Cell **103:** 1033–1045.

Rebay, I., F. Chen, F. Hsiao, P. A. Kolodziej, B. H. Kuang *et al.*, 2000 A genetic screen for novel components of the Ras/Mitogen-activated protein kinase signaling pathway that interact with the yan gene of Drosophila identifies split ends, a new RNA recognition motif-containing protein. Genetics **154:** 695–712.

Reis, R., T. Feijao, S. Gouveia, A. J. Pereira, I. Matos *et al.*, 2009 Dynein and Mast/Orbit/CLASP have antagonistic roles in regulating kinetochore-microtubule plus-end dynamics. J. Cell Sci. **122:** 2543–2553.

Rhee, J., N. S. Mahfooz, C. Arregui, J. Lilien, J. Balsamo *et al.*, 2002 Activation of the repulsive receptor Roundabout inhibits N-cadherin-mediated cell adhesion. Nat. Cell Biol. **4:** 798–805.

Rigaut, G., A. Shevchenko, B. Rutz, M. Wilm, M. Mann *et al.*, 1999 A generic protein purification method for protein complex characterization and proteome exploration. Nat. Biotechnol. **17:** 1030–1032.

Rodriguez, O. C., A. W. Schaefer, C. A. Mandato, P. Forscher, W. M. Bement *et al.*, 2003 Conserved microtubule-actin interactions in cell movement and morphogenesis. Nat. Cell Biol. **5:** 599–609.

Rogers, S. L., U. Wiedemann, U. Hacker, C. Turck and R. D. Vale, 2004 Drosophila RhoGEF2 associates with microtubule plus ends in an EB1-dependent manner. Curr. Biol. **14:** 1827–1833.

Rutishauser, U., 1985 Influences of the neural cell adhesion molecule on axon growth and guidance. J. Neurosci. Res. **13:** 123–131.

Schaefer, A. W., N. Kabir and P. Forscher, 2002 Filopodia and actin arcs guide the assembly and transport of two populations of microtubules with unique dynamic parameters in neuronal growth cones. J. Cell Biol. **158:** 139–152.

Schejter, E. D., and E. Wieschaus, 1993 Functional elements of the cytoskeleton in the early Drosophila embryo. Annu. Rev. Cell Biol. **9:** 67–99.

Shalaby, N. A., A. L. Parks, E. J. Morreale, M. C. Osswalt, K. M. Pfau *et al.*, 2009 A screen for modifiers of notch signaling

uncovers amun, a protein with a critical role in sensory organ development. Genetics **182:** 1061–1076.

Shannon, P., A. Markiel, O. Ozier, N. S. Baliga, J. T. Wang *et al.*, 2003 Cytoscape: a software environment for integrated models of biomolecular interaction networks. Genome Res. **13:** 2498–2504.

Simon, M. A., D. D. Bowtell, G. S. Dodson, T. R. Laverty and G. M. Rubin, 1991 Ras1 and a putative guanine nucleotide exchange factor perform crucial steps in signaling by the sevenless protein tyrosine kinase. Cell **67:** 701–716.

Simpson, J. H., K. S. Bland, R. D. Fetter and C. S. Goodman, 2000 Short-range and long-range guidance by Slit and its Robo receptors: a combinatorial code of Robo receptors controls lateral position. Cell **103:** 1019–1032.

Sousa, A., R. Reis, P. Sampaio and C. E. Sunkel, 2007 The Drosophila CLASP homologue, Mast/Orbit regulates the dynamic behaviour of interphase microtubules by promoting the pause state. Cell Motil. Cytoskeleton **64:** 605–620.

St Johnston, D., 2002 The art and design of genetic screens: Drosophila melanogaster. Nat. Rev. Genet. **3:** 176–188.

Therrien, M., D. K. Morrison, A. M. Wong and G. M. Rubin, 2000 A genetic screen for modifiers of a kinase suppressor of Ras-dependent rough eye phenotype in Drosophila. Genetics **156:** 1231–1242.

Thibault, S. T., M. A. Singer, W. Y. Miyazaki, B. Milash, N. A. Dompe *et al.*, 2004 A complementary transposon tool kit for Drosophila melanogaster using P and piggyBac. Nat. Genet. **36:** 283–287.

Tsvetkov, A. S., A. Samsonov, A. Akhmanova, N. Galjart and S. V. Popov, 2007 Microtubule-binding proteins CLASP1 and CLASP2 interact with actin filaments. Cell Motil. Cytoskeleton **64:** 519–530.

Van Etten, R. A., 1999 Cycling, stressed-out and nervous: cellular functions of c-Abl. Trends Cell Biol. 9: 179–186.

Van Vactor, D., and C. Kopczynski, 1999 Techniques for anatomical analysis of the Drosophila embryonic nervous system, pp. 490–513 in *A Comparative Methods Approach to the Study of Oocytes and Embryos*, edited by J. Richter. Oxford University Press, New York.

Veraksa, A., A. Bauer and S. Artavanis-Tsakonas, 2005 Analyzing protein complexes in Drosophila with tandem affinity purification-mass spectrometry. Dev. Dyn. **232:** 827–834.

Watanabe, T., J. Noritake, M. Kakeno, T. Matsui, T. Harada *et al.*, 2009 Phosphorylation of CLASP2 by GSK-3beta regulates its interaction with IQGAP1, EB1 and microtubules. J. Cell Sci. **122:** 2969–2979.

Wills, Z., L. Marr, K. Zinn, C. S. Goodman and D. Van Vactor, 1999 Profilin and the Abl tyrosine kinase are required for motor axon outgrowth in the Drosophila embryo. Neuron **22:** 291–299.

Wills, Z., M. Emerson, J. Rusch, J. Bikoff, B. Baum *et al.*, 2002 A Drosophila homolog of cyclase-associated proteins collaborates with the Abl tyrosine kinase to control midline axon pathfinding. Neuron **36:** 611–622.

Xu, T., I. Rebay, R. J. Fleming, T. N. Scottgale and S. Artavanis-Tsakonas, 1990 The Notch locus and the genetic circuitry involved in early Drosophila neurogenesis. Genes Dev. **4:** 464–475.

Zhou, F. Q., and C. S. Cohan, 2004 How actin filaments and microtubules steer growth cones to their targets. J. Neurobiol. **58:** 84–91.

Communicating editor: R. Anholt

GENETICS

Supporting Information
http://www.genetics.org/cgi/content/full/genetics.110.115626/DC1

Parallel Genetic and Proteomic Screens Identify Msps as a CLASP-Abl Pathway Interactor in Drosophila

L. A. Lowery, H. Lee, C. Lu, R. Murphy, R. A. Obar, B. Zhai, M. Schedl, D. Van Vactor and Y. Zhan

DOI: 10.1534/genetics.110.115626

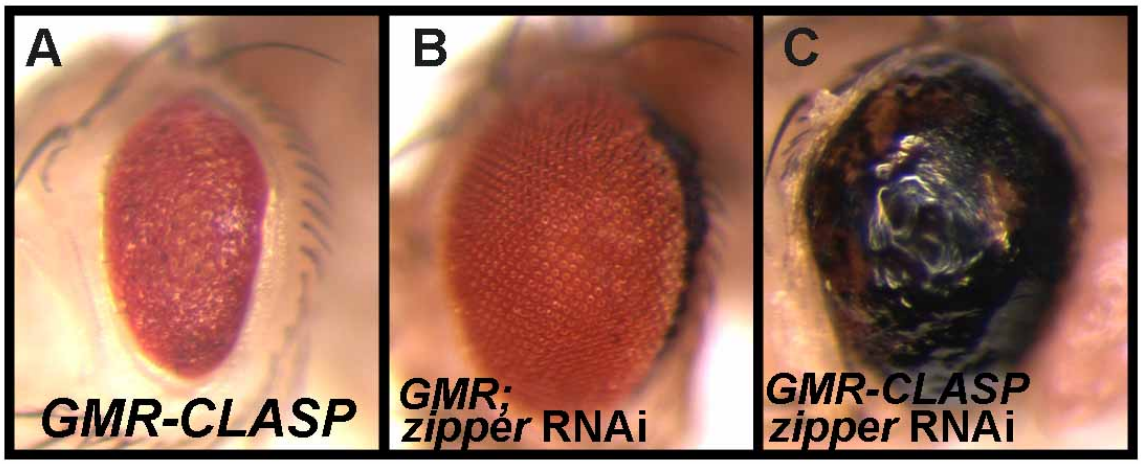

FIGURE S1.—*CLASP* shows very strong interaction with *zipper* in the Drosophila retina. A) Retinal over-expression of *CLASP* (*GMR-GAL4, UAS-CLASP*) induces a rough eye phenotype. (B) Retinal RNAi knock-down of *zipper* (*GD1566*) leads to a mostly wild-type eye with a crescent of abnormal development (right side of eye in figure). (C) Retinal over-expression of *CLASP* combined with RNAi knock-down of *zipper* leads to an eye of normal size but severely disrupted pattern.

TABLE S1

List of CLASP-Interacting Deficiencies

BL ID#	Exel ID#	Interaction	Estimated Cytology	Coordinates
7774	Df(2L)Exel8003	E	21E2;21E2	2L:559139;715085
8000	Df(2L)Exel6006	S	22B5;22D1	2L:1911627;2175599
7495	Df(2L)Exel6009	S	24C3;24C8	2L:3771368;3888977
7504	Df(2L)Exel6018	S	28B1;28C1	2L:7576630;7702880
7820	Df(2L)Exel8026	E	31F5;32B3	2L:10516675;10861982
7510	Df(2L)Exel6027	E	32D2;32D5	2L:11067029;11155825
7515	Df(2L)Exel6032	S	33C2;33D4	2L:12066846--12066969;12270844
7852	Df(2L)Exel7079	S	38E9;38F3	2L:20770538;20874804
7534	Df(2R)Exel6052	S	43C5;43E5	2R:3380702;3510588
7535	Df(2R)Exel6053	S	43D3;43E9	2R:3421058;3553300
7859	Df(2R)Exel7094	E	44A4;44B3	2R:3948670;4019248
7860	Df(2R)Exel7095	E	44B3;44C2	2R:4012164;4119968
7539	Df(2R)Exel6057	S	44B8;44C4	2R:4062156;4214936
7863	Df(2R)Exel8047	S	44D4;44D5	2R:4487805;4536994
7541	Df(2R)Exel6059	S	47C5;47D6	2R:6761890;7073443--7073552
7543	Df(2R)Exel6061	S	48F1;49A6	2R:8149005;8324950
7544	Df(2R)Exel6062	S	49E6;49F1	2R:8868689;8922684
7873	Df(2R)Exel7128	E	50C5;50C9	2R:9689461;9785332
7749	Df(2R)Exel6284	S	51B1;51C2	2R:10462255;10653073--10653275
7882	Df(2R)Exel7137	S	52A13-14;52C8	2R:11463390--11466117;11746753
7549	Df(2R)Exel6067	E	55F8;55F8	2R:14745547;14834784
7554	Df(2R)Exel6072	S	57B16;57D4	2R:16944303;17138350
7553	Df(2R)Exel6071	S	57B3;57B16	2R:16723538;16944303
7998	Df(2R)Exel7166	E	57B3;57B5	2R:16758362;16887668
7900	Df(2R)Exel7169	E	58A3;58B1	2R:17749738--17749756;17927135
7908	Df(2R)Exel7178	E	59D5;59D10	2R:19179008;19283437
7561	Df(2R)Exel6082	E	60C4;60C7	2R:20145420;20257300
7563	Df(3L)Exel6084	S	61B2;61C1	3L:180193;346863
7574	Df(3L)Exel6095	S	63E1;63E3	3L:3460609;3545153
7581	Df(3L)Exel6102	S	64B13;64C4	3L:4692405;4976311
7923	Df(3L)Exel9058	E	64B9;64B9	3L:4542105;4554415
7927	Df(3L)Exel7210	E	65A1;65A5	3L:5919748;6058752
7929	Df(3L)Exel8104	S	65F7;66A4	3L:7353086;7522363
7930	Df(3L)Exel9034	S	66A22;66B3	3L:7974043--7974423;8048609
7933	Df(3L)Exel9048	E	67D1;67D2	3L:9896122;9957205
7595	Df(3L)Exel6116	S	68F2;69A2	3L:12074955;12197081

7601	Df(3L)Exel6122	S	70D4;70D4	3L:14266160;14402934
7609	Df(3L)Exel6130	E	73B5;73D1	3L:16654391;16799748
7935	Df(3L)Exel9002	S	73D1;73D1	3L:16799740--16799741;16837972
7937	Df(3L)Exel9004	E	73D1;73D5	3L:16819356;16888710
7610	Df(3L)Exel6131	E	74A1;74A1	3L:17231345;17414638
7613	Df(3L)Exel6134	E	75C7;75D4	3L:18456353;18615556
7944	Df(3L)Exel9009	S	76B5;76B9	3L:19502738;19628895
7615	Df(3L)Exel6136	E	77B2;77C6	3L:20303330;20486308
7951	Df(3R)Exel9029	S	83A1;83A3	3R:1229919--1229920;1263319
7955	Df(3R)Exel9036	S	85D11;85D11	3R:5152997;5165728
7634	Df(3R)Exel6155	S	85F1;85F10	3R:5754513;5915180
7956	Df(3R)Exel7305	S	86C6;86C7	3R:6606276;6697983
7959	Df(3R)Exel7308	S	86D9;86D9	3R:7069685;7264869
7641	Df(3R)Exel6162	S	87A1;87B5	3R:7713466;8106805
7647	Df(3R)Exel6168	S	87E3;87E8	3R:9105453;9205505--9205506
7649	Df(3R)Exel6170	S	87F10;87F14	3R:9509964--9509965;9638552
7648	Df(3R)Exel6169	E	87F2;87F10	3R:9369363;9509679
7976	Df(3R)Exel8159	S	88A4;88B1	3R:9809236;10085649
7977	Df(3R)Exel7321	S	88A9;88B1	3R:9951211;10103926
7651	Df(3R)Exel6172	E	88D5;88D7	3R:10643950;10743982
7653	Df(3R)Exel6174	S	88F1;88F7	3R:11154443--11154444;11363188
7983	Df(3R)Exel7328	E	89A12;89B6	3R:11835140;11983178
7736	Df(3R)Exel6269	S	89B12;89B18	3R:12131435;12328454
7657	Df(3R)Exel6178	S	90F4;91A5	3R:13992149;14223078
7660	Df(3R)Exel6181	E	91C5;91D5	3R:14566190;14749745
7670	Df(3R)Exel6191	E	94A6;94B2	3R:18193695;18356502
7673	Df(3R)Exel6194	S	94F1;95A4	3R:19210900;19467128
7674	Df(3R)Exel6195	S	95A4;95B1	3R:19467128;19549624
7678	Df(3R)Exel6199	E	95F8;96A2	3R:20096927;20275677
7680	Df(3R)Exel6201	S	96C2;96C4	3R:20963561;21022720
7682	Df(3R)Exel6203	E	96E2;96E6	3R:21341620;21463598
7726	Df(3R)Exel6259	S	98C4;98D6	3R:24152465;24426897

BL = Bloomington Stock Center; Exel ID = Exelixis Deficiency allele name;

E = enhancement of Orbit gain-of-function (GOF) phenotype; S = suppression of CLASP GOF phenotype.

Cytology and coordinates are from Bloomington Stock Center website.

TABLE S2

List of genes with corresponding Exelixis transposon alleles that were uncovered by interacting Dfs

Red bold text designates confirmed interaction (also presented in Table 1). The 68 interacting Deficiencies uncovered a total of 1174 confirmed or predicted genes. Only the 376 genes that had available Exelixis insertion stocks are included in this Table. (Note- 68% of the genes without Exelixis insertions are uncharacterized CGs.) This list contains 699 Exelixis alleles that we screened for interaction, as well as an additional 62 extant non-Exelixis alleles (representing 29 more genes).

14-3-3 (c06705, e00326, e03838, f05080, 2B10)

Aats-met (c00449)

aats-thr (f05143)

AICR2 (f03116, MB017540)

aif (e04281)

akirin (c01011, e00173, e02729, f02419, EY08097)

akt1 (c02098)

aop (c00225, c00266, c06688, c07151, c07184, d00761, **d08252**, d10059, e00003)

aret (c00280, d03152, d07449, d10582, e02519, f02288, f03220, f03620, f04157, f04361)

armi (72.1)

art4 (c06244)

Asf1 (2)

ash1 (B1, 22)

Atx2 (e00368, 06490)

aur (EY03490)

ave (f00865)

az2 (f00932, f07063)

beat-IV (f02545, MB04480)

beat-VI (f05694)

blot (f02653, 01658)

blow (c03280)

boca (d09635, f03889, f05482)

bowl (d08230, d05505)

brwd3 (e00263, f03026, f03832, 05842)

bs (d01376, d05493)

btsz (c04745, d08989)

cad74A (f00312)

Cad86C (MB01251)

cad87A (PL00399)

cad89D (e03186)

cag (f02147)

Cam (**d09785**)

capu (c03227, d05064, **d10743**, **e01050**, f02268)

cdm (BG02608)

ced-12 (c06760)

cht4 (A307)

cht5 (c04908)

comr (f05595)

cona (f04903)

corin (d06364, MB02295)

crumbs (c04784, d02006, f01837, f05973)

csn5 (L4032)

cyp313a2, a3, and a5 (e01417, f05730)

cyt-b5 (d07159, 00681a)

dab (**d11255**, EY10190)

danr (d08076, d10197)

decay (d07129)

Dhc64C (6-10)

dhc98D (MB03402)

didum (KG04384)

DIP2 (f04555)

Dip-B (d06483)

dlc90F (f06010, 04091)

dopR (f02676, PL00420)

dpr15 (f01581)

dpr17 (f05237, f05237, f07135)

ds (c01777, c02476, d05442, e02503, e03049)

E(bx) (c04498, **d02664**, f00603, f03002, Nurf301-3, Nurf301-4)

easter (d09303, d01616)

ect3 (f06233)

eIF-1A (c04533)

eIF2B (c06554, c01931, f00294)

Eip63E (c02102, e00017, e01010, f05185)

epsin-like (d06591)

erf1 (d01190)

est-6 (0)

fer2 (e03248)

fili (d10791, e02018, e04279, f02418, f04573)

fkh (1, 6)

fl(2)d (d02521, e00135, f01270, f04732)

flf1 (d07513)

foxo (c01841, f00765)

frizzled (c05547, d01490, e00573, e01331, e01695, e03401, f00972, f06745, f06941)

fumble (c00596, e03451, f05008)

fus (d01437, d08565, e00008, e00399, e01829, e01903, f03873, f04365)

Fwd (f03822)

galpha73B (c05874)

garz (EP2028, MB05159)

gef64C (c01254, c05011, c05499, e00026, f06164)

gfat2 (c02641)

glass (60j)
glycogenin (d00632, f07729)
glyp (d10498)
got2 (d06666)
gsc (d06023, f02129, f03339)
gwl (f04701, EP515)
gyc32E (e02623)
gyc-89Da (e01821)
gyk (e00237)
IM4 (c06403)
Ipk (f06675)
Ipk2 (f02238)
ir94d (f05980)
jheh3 (EY09329)
kermit (d06406)
king-tubby (d03644)
kp78a (c02917, d07016)
kp78b (c02917, d07016)
l(2)k16918 (c01866, c04665, c05834, c06253, d02844, e02160, f06545)
l(3)j2D3 (e01532)
larp (d00350, e00508, f01093, f01481)
Lasp (c00600, c04231, c05029, e00056, e03191, e03659, f02610)
lig (d01556, e01589, e04268, f03269)
lip2 (f06907)
lip4 (f07089)
lkb1 (f01125)
Lmpt (c00274, c00698, c01851, c03100, c04937, c04940, d01744, d02928, d06017, e04493, f00569, f01879, f05277)
lrr47 (e00177)
luna (c02278, c02488, c06554, c06758, e01606, e02825, f03787, f04294, f05588, f07504)
lush (f03787)
mats (e03077, e03078)
Mekk1 (**d01115**, d04302, e01939, f06987)
met75Ca (f00316)
mhcl (c05149, e03696)
MICAL (c00824, c03080)
miple (c05178)
mlh1 (c00143, e00130)
moca-cyp (EY06157, KG10533)
mRpL15 (e03567, KG06809)
mRpL9 (c00642, c01361, c01447, e00553, e00554, e02746, f00687)
mRpS33 (f01766, f01785)
msi (c01658, d08770, f00965, f01082, f07665, EY07912)
mspo (f04337, f04549)
msps (**c03283, d03376**)
mtch (e00205)
mthl10 (f01047)
mthl14 (e04476, f00733)
myo28B1 (f01484)
ninaG (e00313)
nmo (c00439, c05873)
nos (c01670, e02671, f02274, f02469)
not (d04543, d06314, 02069)
npc2 (**d04217**)
Nrt (c04672, e02875, f02550, f04653)
Nrx-1 (c03581, d08766)
nrx-IV (4304)
nudC (c03957, c02110, c04337, f05219, PL00420)
nup107 (c01031)
nup160 (f07177)
oa2 (f02819)
obp44a (f02697)
or49a (e02161)
or83b (1)
otp (f03917)
pabp2 (d09497)
pad (d03595)
pak3 (d02472)
patsas (f05143)
pinta (1)
pnr (f04283)
pnut (**c04668**, e02510)
poly (d04286, e02734, f01552)
porin (f03616)
pp2a-b' (**c00535**, c04846)
pph13 (f03236)
pros (10419)
psn (9)
Pu (e02190, f06584)
pyk (d05514, d05959, f06019)
pyx (c04447)
rab6 (f05135)
rac2 (d01612, delta)
rbp1 (e01298, e02960, e04474)
rbp4 (f05744)
rdx (c02298, c04993, c06670, d01317, d02587, d05421, d08815, d09180, f04694)
repo (03702)
Rfc38 (e00704, **f07177**)
rgr (e02986, f04327)
rh4 (c04779)
Rh7 (c00019, c04281, f01103)
rho-6 (e01596)
rhoBTB (e02774, EP3099)
RhoGEF3 (c01758, f03039)
rin (1, 2)

rpb4 (e04115)
rpn6 (c01311, c04402, f00865)
rpp6 (f07001)
sano (c00519, c01291, c01392, c04142, d09385, **d10230**, f07766)
scra (c01769, c01770)
sec63 (e03550, f01027, EY04730)
SF2 (d03595)
sh3beta (MB03704)
shal (f00495, f00700, MB05249)
shot (c00857, c01025, c03247, c05431, c07162, **d00747**, d02359, d02801, d03296, d05068, d05163, d06144, d08375, d09913, f06882, f07764)
sina (c04779, 3)
sip2 (d09417, f07564)
slbo (d11553)
slob (d07006, e04189)
slp1 (d07508)
slv (d07339, e00541, e00809)
smid (c02443)
smsr (f01601)
snap (G8)
socs44a (f07030)
spn (c06515, d06681, e03547, f01597)
squid (c04803, e01416, f01931)
ss (f03362, f07846, a)
ssdp (d03345, e03097)
stam (e00677)
star1 (f03415)
stj (c01305, e01058, f00903)
stwl (e01521)
su(dx) (**f02193**)
Su(var)2-HP2 (e02091)
su(z)2 (e00448, **f07746**)
Surf4 (EY139940)
sut1 (d07339, EY12588)
svp (c03526, d02075, e04490, f02985)
synaptogyrin (c06556)
Taf5 [EY01764b]
Taf6 (f06930, 1)
task6 (f01884, EY23668)
t-cp1 (c03987)
tepII (f02756)
term (f03837)
tho2 (c02867, e03823)
thoc6 (e00363)
thoc7 (d05792)
tk (c01416, f03824, f06233)
Toll-9 (c05666)
tra2 (**d10032**)
treh (d01034, d03022)
tribbles (**d03175**, d03251, d07751)
trim9 (c02205, e04684)
trx (c00678, c07009, d00566, d01427, d08983, e00972, e01275)
TSG101 (f00976)
ttm2 (c05054, d10863)
tudor (c00814, e04651, f02752)
twf (c04422)
ubcD2 (c01581, e01595)
vari (d10880, d11181, e01914, f00033)
vha100-2 (d00417)
vha14 (c01762, f03593)
vhaPPA1-1 (e03223)
vps13 (c03628)
wac (c00217, e01983)
wallenda (c00701, d09171, e01933, **f00690**)
WRNexo (e04496)
xbp1 (d08698)
yps (c01240)
zasp (c00557, e04254, f00107, f04847)
zip3 (d00961)
CG10139 (c01615, c01709, c05462)
CG10168 (f03105)
CG10254 (c01359, c06687, e03373)
CG10479 (d08677)
CG10543 (d05245)
CG11357 (c07045, f06786)
CG11723 (c02850)
CG12250 (c05082)
CG12391 (e00914)
CG12413 (c02868, f07617)
CG12736 (f00932)
CG12753 (f07675)
CG12857 (d01332)
CG12869 (c06468)
CG13025 (e03112)
CG13031 (e02987)
CG13155 (f03327)
CG13344 (c05436)
CG13380 (f03512)
CG13551 (e03979, e04159)
CG1358 (e02192, e04134, f05605)
CG13689 (e00773)
CG13847 (c04266)
CG13875 (d10431)
CG14292 (f04985)
CG14357 (e01192)
CG14669 (c06402)
CG14687 (c02737, c02742)

CG14693 (f03110)
CG14731 (c04833)
CG14756 (f04886)
CG14869 (c03231)
CG14879 (c04676, c06597, f06730)
CG14894 (f04937)
CG14899 (c01405, c01411)
CG14921 (d05080)
CG14971 (c02743)
CG15658 (f06836)
CG1602 (e01855, f05157)
CG1603 (f04743)
CG16971 (c02583, d10202, e03102)
CG17086 (e02595)
CG17118 (f07762)
CG17124 (c01575, f03842)
CG17150 (f03522)
CG17153 (c00543)
CG17565 (c00570)
CG17836 (c00560, c00620, c02198)
CG17931 (f00467)
CG18208 (f03483)
CG18347 (e03533)
CG18375 (e02134, e02586, f00807)
CG18547 (d05047)
CG1894 (f06204)
CG2144 (e01855, f05157)
CG2158 (e02135)
CG2813 (f02238, f02290, f05607)
CG30016 (f02466)
CG30020 (f02147)
CG30090 (f06357)
CG30373 (e01825)
CG30389 (d04848, f04544)
CG30414 (e03801)
CG30492 (f03610)
CG30499 (f05482)
CG31145 (c01050, e03246)
CG31169 (c05253, c05300, f01116, f07270)
CG31211 (e01498)
CG31301 (f04660)
CG31302 (f07217)
CG31326 (c06214, c06215)
CG31337 (e04105)
CG31386 (f02579)
CG3153 (f04678)
CG31670 (f07652)
CG31673 (e00103, e00764)
CG31674 (d00365)
CG31676 (f05642)
CG31869 (f01438, f06293)
CG31871 (f02763)
CG31957 (f05539)
CG31960 (f02028)
CG32267 (c02100, f01961)
CG32343 (e00358, f03397, f06767)
CG32473 (c01723, e00341, f00509)
CG3281 (f01539)
CG33523 (c03097, c04974, e03176)
CG3376 (d09724)
CG34356 (f04913)
CG34376 (c00435, c01198, d03230)
CG34383 (f01731)
CG34404 (e02686)
CG3493 (c00545, c00551)
CG3530 (d07361)
CG3532 (c03845, e02741)
CG3631 (f00630)
CG3868 (f00601)
CG3925 (f07378)
CG4050 (c03307)
CG4089 (c04500, f00290)
CG42524 (f00129)
CG4266 (c05426)
CG4302 (d03020)
CG4565 (c05681)
CG4673 (f01843)
CG4848 (e02840, f03759, f06192)
CG4860 (f07663)
CG5013 (f04294)
CG5130 (c02029, c04211, c06997)
CG5276 (e03505)
CG5281 (e00749)
CG5346 (e01317)
CG5359 (e03976, f01625, f01900)
CG5618 (f05961)
CG5645 (e03479)
CG5910 (e01524, e02064, e03495)
CG6136 (e02834)
CG6171 (d07444)
CG6192 (c02648)
CG6194 (f01043)
CG6196 (f00985)
CG6201 (d02957, d07625)
CG6218 (d06481)
CG6287 (d01875, d02470, f02402, f07100)
CG6289 (e01796)
CG6347 (e00490)

CG6357 (c00284, d03281)
CG6567 (d04782, d09306)
CG6574 (e00293)
CG6719 (e00315)
CG6724 (c04485, e00942, e02149)
CG6729 (c04960)
CG6739 (d09967, e02971)
CG6744 (c05566, c05871)
CG6750 (e02662)
CG6971 (f06383)
CG7337 (c02558, c04728, e02910, f04537, f05580, f05757)
CG7509 (e02823)
CG7692 (f06961, f07642)
CG7720 (f04152)
CG7985 (f08065)
CG7998 (c06552)
CG8064 (c05886)
CG8712 (e00152, e01489)
CG8713 (e00867)
CG8784 (f01901)
CG8790 (c01293)
CG8795 (f02573)
CG8830 (e00699)
CG8839 (c02700)
CG9286 (f00745)
CG9288 (f00354)
CG9312 (f04951)
CG9328 (e02136, e03944)
CG9330 (f04902)
CG9339 (c04650)
CG9368 (c05889)
CG9611 (e01522)
CG9669 (f07000)
CG9674 (d09764, f04248)
CG9813 (d05235)
CG9918 (f01726)
CG9922 (f01835)

TABLE S3

CLASP-TAP Hits

Symbol	Flybase ID	CG #	Predicted Function[a]	# of experimental identifications	Distinct peptides	Total peptides	Average XCorr
zip	FBgn0005634	CG15792	cytoskeletal	4	162	1156	4.152
jar	FBgn0011225	CG5695	cytoskeletal	4	22	41	3.540
Chd64	FBgn0035499	CG14996	cytoskeletal	4	9	36	3.746
cpb	FBgn0011570	CG17158	cytoskeletal	4	5	10	3.270
CG13366	FBgn0025633	CG13366	cytoskeletal	3	10	15	3.041
bif	FBgn0014133	CG1822	cytoskeletal	3	8	13	3.825
kst	FBgn0004167	CG12008	cytoskeletal	3	8	8	2.532
Gel	FBgn0010225	CG1106	cytoskeletal	3	5	6	3.246
Arp66B	FBgn0011744	CG7558	cytoskeletal	3	2	3	3.408
shot	FBgn0013733	CG18076	cytoskeletal	2	7	7	3.283
msps	FBgn0027948	CG5000	cytoskeletal	1	1	1	3.998
CG3339	FBgn0039510	CG3339	cytoskeletal	1	1	1	2.403
CG14998	FBgn0035500	CG14998	cytoskeletal	1	1	1	3.382
Arpc3A	FBgn0038369	CG4560	cytoskeletal	1	1	1	3.446
Arc-p34	FBgn0032859	CG10954	cytoskeletal	1	1	1	3.426
ctp	FBgn0011760	CG6998	cytoskeletal	1	1	1	3.059
TER94	FBgn0024923	CG2331	cytoskeletal	1	1	1	3.578
Ank2	FBgn0085445	CG34416	cytoskeletal	1	1	1	2.415
Tctp	FBgn0037874	CG4800	cytoskeletal	1	1	1	3.295
spir	FBgn0003475	CG10076	cytoskeletal	1	1	1	2.345
CG5740	FBgn0038932	CG5740	cytoskeletal	1	1	1	3.669
Cam	FBgn0000253	CG8472	receptors and signaling	4	7	28	3.718
Flo	FBgn0024754	CG8200	receptors and signaling	2	4	5	3.173
Pp2A-29B	FBgn0005776	CG17291	receptors and signaling	2	2	3	3.989
CG6453	FBgn0032643	CG6453	receptors and signaling	2	2	2	3.538
bor	FBgn0040237	CG6815	receptors and signaling	2	1	3	4.195
CG4164	FBgn0031256	CG4164	receptors and signaling	2	1	2	3.460
CG11984	FBgn0037655	CG11984	receptors and signaling	2	1	2	5.010
flw	FBgn0000711	CG2096	receptors and signaling	2	1	2	3.402
CG31012	FBgn0027598	CG31012	receptors and signaling	1	2	2	3.333
Past1	FBgn0016693	CG6148	receptors and signaling	1	2	2	3.565
rl	FBgn0003256	CG12559	receptors and signaling	1	2	2	2.457
Abl	FBgn0000017	CG4032	receptors and signaling	1	1	1	2.598
CG17272	FBgn0038830	CG17272	receptors and signaling	1	1	1	3.437
Rab5	FBgn0014010	CG3664	receptors and signaling	1	1	1	3.536
CG17765	FBgn0033529	CG17765	receptors and signaling	1	1	1	2.308

CG13887	FBgn0035165	CG13887	receptors and signaling	1	1	1	2.475
Rtnl1	FBgn0053113	CG33113	receptors and signaling	1	1	1	2.212
vlc	FBgn0010633	CG8390	receptors and signaling	1	1	1	2.391
CG17090	FBgn0035142	CG17090	receptors and signaling	1	1	1	2.219
gig	FBgn0005198	CG6975	receptors and signaling	1	1	1	3.062
Ranbp9	FBgn0037894	CG5252	receptors and signaling	1	1	1	3.576
c11.1	FBgn0040236	CG12132	receptors and signaling	1	1	1	4.043
CalpB	FBgn0025866	CG8107	receptors and signaling	1	1	1	2.268
Hml	FBgn0029167	CG7002	receptors and signaling	1	1	1	3.666
Sara	FBgn0026369	CG15667	receptors and signaling	1	1	1	3.397
CG5168	FBgn0032246	CG5168	receptors and signaling	1	1	1	2.395
hig	FBgn0010114	CG2040	receptors and signaling	1	1	1	2.451
scb	FBgn0003328	CG8095	receptors and signaling	1	1	1	2.202
Flo-2	FBgn0024753	CG32593	receptors and signaling	1	1	1	4.290
Pp1alpha-96A	FBgn0003134	CG6593	receptors and signaling	1	1	1	2.548
CanA1	FBgn0010015	CG1455	receptors and signaling	1	1	1	2.813
CG3530	FBgn0028497	CG3530	receptors and signaling	1	1	1	3.100
CG10535	FBgn0037926	CG10535	receptors and signaling	1	1	1	3.402
CG1227	FBgn0037491	CG1227	receptors and signaling	1	1	1	2.981
CG7891	FBgn0037551	CG7891	receptors and signaling	1	1	1	3.411
Arf79F	FBgn0010348	CG8385	receptors and signaling	1	1	1	2.328
Gtp-bp	FBgn0010391	CG2522	receptors and signaling	1	1	1	4.782
R	FBgn0004636	CG1956	receptors and signaling	1	1	1	3.658
Rab2	FBgn0014009	CG3269	receptors and signaling	1	1	1	2.757
Ef1alpha48D	FBgn0000556	CG8280	mRNA reg/translation	4	9	24	3.271
sop	FBgn0004867	CG5920	mRNA reg/translation	3	5	8	3.164
sqd	FBgn0003498	CG16901	mRNA reg/translation	3	5	6	3.610
Qm	FBgn0024733	CG17521	mRNA reg/translation	3	4	5	3.026
growl	FBgn0037245	CG14648	mRNA reg/translation	2	4	10	3.187
eIF3-S10	FBgn0037249	CG9805	mRNA reg/translation	2	3	3	3.040
Rm62	FBgn0003261	CG10279	mRNA reg/translation	2	3	3	3.143
CG4225	FBgn0038376	CG4225	mRNA reg/translation	2	1	2	3.625
AGO2	FBgn0046812	CG7439	mRNA reg/translation	1	3	3	4.021
larp	FBgn0040108	CG14066	mRNA reg/translation	1	2	3	3.912
aub	FBgn0000146	CG6137	mRNA reg/translation	1	2	2	3.363
pit	FBgn0025140	CG6375	mRNA reg/translation	1	1	2	2.774
Fmr1	FBgn0028734	CG6203	mRNA reg/translation	1	1	1	3.612
Srp72	FBgn0038810	CG5434	mRNA reg/translation	1	1	1	4.242
Srp68	FBgn0035947	CG5064	mRNA reg/translation	1	1	1	2.767
Aats-asp	FBgn0002069	CG3821	mRNA reg/translation	1	1	1	2.337
CG31739	FBgn0051739	CG31739	mRNA reg/translation	1	1	1	2.961

Aats-asn	FBgn0086443	CG10687	mRNA reg/translation	1	1	1	3.489
Rs1	FBgn0021995	CG2173	mRNA reg/translation	1	1	1	3.669
CG1972	FBgn0039691	CG1972	mRNA reg/translation	1	1	1	2.390
CG16940	FBgn0035111	CG16940	mRNA reg/translation	1	1	1	3.323
Atx2	FBgn0041188	CG5166	mRNA reg/translation	1	1	1	2.637
nop5	FBgn0026196	CG10206	mRNA reg/translation	1	1	1	2.439
CG30122	FBgn0050122	CG30122	mRNA reg/translation	1	1	1	2.170
CG10777	FBgn0029979	CG10777	mRNA reg/translation	1	1	1	2.683
CG8235	FBgn0033351	CG8235	mRNA reg/translation	1	1	1	5.473
rin	FBgn0015778	CG9412	mRNA reg/translation	1	1	1	2.250
Hrb98DE	FBgn0001215	CG9983	mRNA reg/translation	1	1	1	2.675
mub	FBgn0014362	CG7437	mRNA reg/translation	1	1	1	2.753
Hel25E	FBgn0014189	CG7269	mRNA reg/translation	1	1	1	2.206
bonsai	FBgn0026261	CG4207	mRNA reg/translation	1	1	1	2.619
Ef1beta	FBgn0028737	CG6341	mRNA reg/translation	1	1	1	3.243
CG8578	FBgn0030699	CG8578	DNA binding/transcription	4	9	23	3.813
ref(2)P	FBgn0003231	CG10360	DNA binding/transcription	2	3	3	2.750
Pep	FBgn0004401	CG6143	DNA binding/transcription	2	1	2	4.724
DNApol-delta	FBgn0012066	CG5949	DNA binding/transcription	1	2	2	2.391
yps	FBgn0022959	CG5654	DNA binding/transcription	1	2	2	3.040
CG7380	FBgn0031977	CG7380	DNA binding/transcription	1	2	2	4.073
CG3838	FBgn0032130	CG3838	DNA binding/transcription	1	1	1	3.625
CG13350	FBgn0033890	CG13350	DNA binding/transcription	1	1	1	3.886
His1	FBgn0053831	CG33831	DNA binding/transcription	1	1	1	4.128
glu	FBgn0015391	CG11397	DNA binding/transcription	1	1	1	2.714
lat	FBgn0005654	CG4088	DNA binding/transcription	1	1	1	2.738
psq	FBgn0004399	CG2368	DNA binding/transcription	1	1	1	2.821
Z4	FBgn0037066	CG7752	DNA binding/transcription	1	1	1	3.596
mor	FBgn0002783	CG18740	DNA binding/transcription	1	1	1	2.466
Taf11	FBgn0011291	CG4079	DNA binding/transcription	1	1	1	2.498
bic	FBgn0000181	CG3644	DNA binding/transcription	1	1	1	2.440
Top2	FBgn0003732	CG10223	DNA binding/transcription	1	1	1	2.375
HDAC4	FBgn0041210	CG1770	DNA binding/transcription	1	1	1	3.421
Pfk	FBgn0003071	CG4001	metabolism	3	2	4	2.544
Scs-fp	FBgn0017539	CG17246	metabolism	3	2	3	3.768
l(2)03709	FBgn0010551	CG15081	metabolism	2	2	2	3.956
CG6439	FBgn0038922	CG6439	metabolism	1	3	3	3.443
l(1)G0156	FBgn0027291	CG12233	metabolism	1	3	3	3.411
CG31694	FBgn0051694	CG31694	metabolism	1	2	2	4.753
CG4050	FBgn0020312	CG4050	metabolism	1	1	1	2.668
CG12264	FBgn0032393	CG12264	metabolism	1	1	1	3.863

Cyp6a23	FBgn0033978	CG10242	metabolism	1	1	1	2.695
CG3797	FBgn0036842	CG3797	metabolism	1	1	1	2.332
Gfat2	FBgn0039580	CG1345	metabolism	1	1	1	2.435
Mgstl	FBgn0025814	CG1742	metabolism	1	1	1	2.684
CG3714	FBgn0031589	CG3714	metabolism	1	1	1	3.507
CG1516	FBgn0027580	CG1516	metabolism	1	1	1	3.185
Sply	FBgn0010591	CG8946	metabolism	1	1	1	4.342
CG42261	FBgn0259146	CG42261	metabolism	1	1	1	2.801
CG15533	FBgn0039768	CG15533	metabolism	1	1	1	2.804
CG14482	FBgn0034245	CG14482	metabolism	1	1	1	2.242
CG4729	FBgn0036623	CG4729	metabolism	1	1	1	2.812
v(2)k05816	FBgn0042627	CG3524	metabolism	1	1	1	3.086
CG9384	FBgn0036446	CG9384	metabolism	1	1	1	2.309
CG15820	FBgn0035312	CG15820	metabolism	1	1	1	2.214
CG7335	FBgn0036941	CG7335	metabolism	1	1	1	2.269
OstStt3	FBgn0011336	CG7748	metabolism	1	1	1	3.669
Pcmt	FBgn0015276	CG2152	metabolism	1	1	1	2.965
CG6283	FBgn0039474	CG6283	metabolism	1	1	1	2.211
CG12030	FBgn0035147	CG12030	metabolism	1	1	1	3.326
alt	FBgn0038535	CG18212	lipid particle	2	2	3	4.105
kuk	FBgn0038476	CG5175	lipid particle	1	1	2	3.802
l(2)37Cc	FBgn0002031	CG10691	lipid particle	1	2	2	4.072
CG2158	FBgn0033264	CG2158	protein transport	2	1	2	3.876
shrb	FBgn0086656	CG8055	protein transport	1	2	2	4.145
Karybeta3	FBgn0011341	CG1059	protein transport	1	2	2	2.575
CG11779	FBgn0038683	CG11779	protein transport	1	1	1	2.572
ALiX	FBgn0086346	CG12876	protein transport	1	1	1	2.301
Chmp1	FBgn0036805	CG4108	protein transport	1	1	1	2.807
Vha100-3	FBgn0028669	CG30329	ion transport	1	1	1	2.377
CG15270	FBgn0028879	CG15270	ion transport	1	1	1	2.433
Ir75a	FBgn0036757	CG14585	ion transport	1	1	1	2.373
l(1)G0230	FBgn0028342	CG2968	ion transport	1	1	1	3.032
CG31860	FBgn0051860	CG31860	ion transport	1	1	1	2.313
AP-47	FBgn0024833	CG9388	synaptic vesicle	1	1	1	2.482
AP-50	FBgn0024832	CG7057	synaptic vesicle	1	1	1	3.411
AP-1gamma	FBgn0030089	CG9113	synaptic vesicle	1	1	1	2.384
alphaCop	FBgn0025725	CG7961	synaptic vesicle	1	1	1	2.221
Rpt4	FBgn0028685	CG3455	proteolysis	1	2	2	3.026
Pros26.4	FBgn0015282	CG5289	proteolysis	1	1	1	3.720
CG8209	FBgn0035830	CG8209	proteolysis	1	1	1	2.244
CG8492	FBgn0035813	CG8492	proteolysis	1	1	1	2.214

faf	FBgn0005632	CG1945	proteolysis	1	1	1	2.267
CG7033	FBgn0030086	CG7033	protein folding	1	1	1	3.638
CG18259	FBgn0030956	CG18259	DNA replication	1	1	1	3.715
CG42354	FBgn0259700	CG42354	unknown	1	1	1	4.704
CG5953	FBgn0032587	CG5953	unknown	1	1	1	3.167
CG11844	FBgn0046214	CG11844	unknown	1	1	1	2.950
CG5217	FBgn0038694	CG5217	unknown	1	1	1	2.672
CG31955	FBgn0051955	CG31955	unknown	1	1	1	2.660
CG17362	FBgn0036393	CG17362	unknown	1	1	1	2.552
CG5515	FBgn0039163	CG5515	unknown	1	1	1	2.498
CG10185	FBgn0038397	CG10185	unknown	1	1	1	2.489
l(2)s5379	FBgn0010704	CG7085	unknown	1	1	1	2.463
CG11671	FBgn0037562	CG11671	unknown	1	1	1	2.343
CG13326	FBgn0033794	CG13326	unknown	1	1	1	2.209
CG15019	FBgn0035541	CG15019	unknown	1	1	1	3.726
CG14969	FBgn0035440	CG14969	unknown	1	1	1	2.596
CG15625	FBgn0031644	CG15625	unknown	1	1	1	2.444
CG8929	FBgn0034504	CG8929	unknown	1	1	1	2.245
CG15071	FBgn0034377	CG15071	unknown	1	1	1	2.218
CG33978	FBgn0053978	CG33978	unknown	1	1	1	2.241

Distinct Peptides represents the number of distinct peptide sequences observed when combining all four MS experiments.
Total Peptides represents the sum of total peptides observed when combining all four MS experiments.

TABLE S4

List of genes tested for interaction with CLASP (whose corresponding proteins were obtained by the proteomic screen). Exelixis transposon allele(s) are listed below gene. Alleles which showed interaction are in bold red text (S=suppression, E=enhancement). Of the 179 candidate proteins, we tested 84 genes for genetic interaction using Exelixis transposon alleles. (The remaining 96 lines either do not have corresponding Exelixis lines (82) or we were unable to obtain them (13)).

msps
c03283 (E)
d03376 (S)
c00130
f00712

shot
c00857
c01025
c03247
c05431
c07162
d00747 (E)
d01259
d02359
d02801
d03296
d05068
d05163
d06144
d08375
d09913
f06882 (E)
f07764

jar
c04556
d02458
d05397 (S)
f04622

bif
d01104 (S)
d02599 (S)

kst
d11183 (S)
d09063 (S)

Cam
d09785 (S)
c04225
c04229
d01888
f02054

eIF3-S10
e03075 (S)

CG13366
d00293 (S)
d10875
e03915
e04403
f06462
f06515
f08034
d04145
d00293

CG2092
c01769
c01770

zip
d05611
f02948
f07547
GD1566

CG4800
e04436

CG10076
d02631
f00060
f07723

CG17272
e04089 (S)

Rab5
d09675 (S)
d11055
e02885
e03041

CG6453
e02094
f02408

CG17765
f01479

CG8107
c05673
e04062

CG4164
c00496

CG11984
d08881

CG33113
d07427
e04183

CG31012
c01086
f01073

CG7002
f03374

CG5168
c04880
c04956

CG2040
d10310
e00507
f05147
f06695

CG8390
d01566
d01574
e00027

CG8095
f06320

CG8200
e02554

CG17291
f08078

CG1455
f01787

CG3530
d07361

CG10535
c00296

CG1227
c03858
e03081
f02638

CG17090
d07497
d10792
e02695
f04609

CG7891
e00336

CG8385
c06390

CG3269
c02699

Fmr1
d10091 (E)

CG6137
c01100
d04301

CG3821
c02661

CG31739
e01605

CG6375
f06954

CG9805
e03075

CG5166
e00368

CG16901
e01416
f01931

CG7437
d01447
d03166
e00354
e03562
f03532
f03831
f05421

CG14648
c02107
d08462
e00245
f00035

CG7269
e02545

CG5920
d05318

CG5949
e04106

CG10223
c05388
d05357
f05145

CG3838
c02372
f04347

CG10212
f05586

CG13350
e01894

CG11397
f01998

CG2368
c00275
c03083
d04086
d04668
e00746
e00835
e02046
e04681
f01460
f02072
f02627
f03625
f04806

CG7752
c06011

CG5654
c01240

CG6143
c00589
f0513

CG10360
c03993
e00482

CG18212
c04824
d02566
f03755

CG3524
d04154
f02757

CG4001
c06016
c06496
c01155

CG9384
e00564

CG31694
c03550
e03952

CG6439
f07670

CG3714
f07540

CG7748
e03710

CG2152
f00979

CG1516
d00382
d00472
f04160

CG17246
e04630

CG12030
f00624

CG4050
c03307

CG1059
c01681
c02568
c02569
e01997

CG11779
d06728

CG2158
e02135

CG1945
c01838
c06363

CG14066
d00350
e00508
f01093
f01481

CG14998
d02685
f07121
d03634
d04526

CG5515
f02614

CG15625
e03818

CG8055
d02738

CG7462
f00518
f02001

CG12876
e03200
f03094